Microbiome

RESEARCH

Open Access

Bacteroides uniformis degrades *β*-glucan to promote *Lactobacillus johnsonii* improving indole-3-lactic acid levels in alleviating colitis

Shanshan Zhang[1†], Qixing Nie[1†], Yonggan Sun[1†], Sheng Zuo[1], Chunhua Chen[1], Song Li[1], Jingrui Yang[1], Jielun Hu[1], Xingtao Zhou[1], Yongkang Yu[1], Ping Huang[2], Lu Lian[2], Mingyong Xie[1*] and Shaoping Nie[1*]

Abstract

Background Intake of dietary fiber is associated with a reduced risk of inflammatory bowel disease. *β*-Glucan (BG), a bioactive dietary fiber, has potential health-promoting effects on intestinal functions; however, the underlying mechanism remains unclear. Here, we explore the role of BG in ameliorating colitis by modulating key bacteria and metabolites, confirmed by multiple validation experiments and loss-of-function studies, and reveal a novel bacterial cross-feeding interaction.

Results BG intervention ameliorates colitis and reverses *Lactobacillus* reduction in colitic mice, and *Lactobacillus* abundance was significantly negatively correlated with the severity of colitis. It was confirmed by further studies that *Lactobacillus johnsonii* was the most significantly enriched *Lactobacillus* spp. Multi-omics analysis revealed that *L. johnsonii* produced abundant indole-3-lactic acid (ILA) leading to the activation of aryl hydrocarbon receptor (AhR) responsible for the mitigation of colitis. Interestingly, *L. johnsonii* cannot utilize BG but requires a cross-feeding with *Bacteroides uniformis*, which degrades BG and produces nicotinamide (NAM) to promote the growth of *L. johnsonii*. A proof-of-concept study confirmed that BG increases *L. johnsonii* and *B. uniformis* abundance and ILA levels in healthy individuals.

Conclusions These findings demonstrate the mechanism by which BG ameliorates colitis via *L. johnsonii*–ILA–AhR axis and reveal the important cross-feeding interaction between *L. johnsonii* and *B. uniformis*.

Keywords *β*-glucan, Inflammatory bowel disease, *Lactobacillus johnsonii*, *Bacteroides uniformis*, Cross-feeding, Indole-3-lactic acid, Aryl hydrocarbon receptor, Nicotinamide

[†]Shanshan Zhang, Qixing Nie, and Yonggan Sun contributed equally to this work.

*Correspondence:
Mingyong Xie
myxie@ncu.edu.cn
Shaoping Nie
spnie@ncu.edu.cn
Full list of author information is available at the end of the article

Graphical Abstract

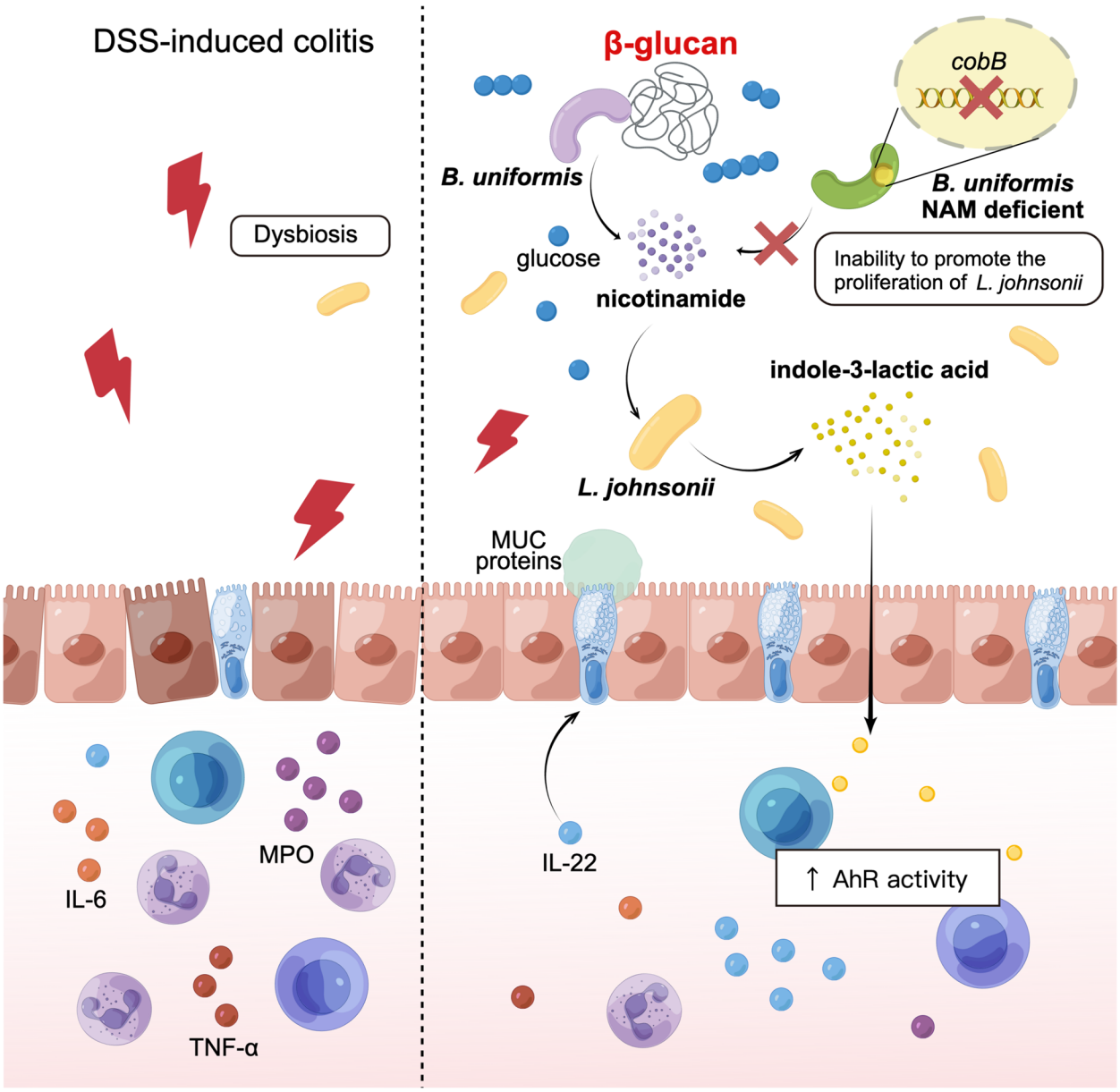

Background

Inflammatory bowel disease (IBD), which includes ulcerative colitis and Crohn's disease, is a chronic inflammatory disorder of the gastrointestinal tract and has affected millions of people worldwide. The development of IBD is believed to result from a complex interplay between genetic, microbial, and environmental factors, with dysbiosis of the gut microbiota playing a central role in its pathogenesis [1]. Diet is a key determinant of microbiota composition [2]. Previous studies have confirmed that dietary fiber intake is associated with a reduced risk of IBD [3].

The dysbiosis of gut microbiota in patients with IBD is characterized by decreased microbial diversity, including the reduced abundance of beneficial microbes, such as *Lactobacillus*, *Bifidobacterium*, and butyrate-producing organisms *Faecalibacterium prausnitzii* [4, 5], and enriched *Ruminococcus gnavus* and adherent invasive *Escherichia coli* [6]. Moreover, alterations in metabolic patterns have been observed in IBD patients [7].

Microbial metabolites play a significant role in the interaction between the gut microbiota and the host, exerting diverse effects on host physiology [8]. Certain metabolites such as short-chain fatty acids (SCFAs), bile acids, and indole derivatives were found significantly changed in patients with IBD, which affect intestinal homeostasis via multiple mechanisms [9]. Among them, many indole derivatives have been reported to modulate intestinal immunity by acting as agonists of the aryl hydrocarbon receptor (AhR), which is often deficient in patients with IBD [10], and supplementation with specific indole derivatives has been found to be beneficial to ameliorate colitis [11]. This suggests that the manipulation of gut microbiota and related metabolites is a promising therapeutic strategy for IBD management. Recent reviews highlight that dietary fiber could help promote the growth of specific commensal microorganisms and produce beneficial metabolites for host health [12, 13]. Exploring the mechanisms by which dietary fiber ameliorates colitis is an important step to advancing this approach as a treatment for IBD.

β-Glucan (BG) is a type of soluble fiber found in various natural sources such as oats, barley, and wheat. It is widely recognized for its potential health benefits and is considered an important dietary component. BG has obtained generally recognized as safe (GRAS) certification, allowing its use as a fiber source in a wide range of food and beverage applications. The American Food and Drug Administration (FDA) issued a health claim stating that intake of oat BG at daily doses of at least 3 g may reduce plasma total and low-density lipoprotein cholesterol levels [14], and BG was approved by the Chinese National Health Commission as a novel food ingredient in 2014. Despite some supportive findings regarding the anti-inflammatory potential of cereal BG [15], its overall evaluation in colitis, impact on the microbiota, and the underlying mechanism have not been elucidated.

In this study, we demonstrated that BG ameliorates colitis in a microbiota-dependent manner. Based on the in vitro fermentation and in vivo animal experiments, the effect of BG on the gut microbiota was characterized by an increased abundance of *L. johnsonii*. Colonization of *L. johnsonii* alleviates colitis by activation of the AhR–IL-22 signaling pathway. We also proved that *L. johnsonii*-derived indole-3-lactic acid (ILA) is a key bioactive metabolite for the activation of AhR. Of note, *L. johnsonii* was unable to directly degrade BG, and its proliferation was facilitated by *Bacteroides uniformis* and its metabolite, nicotinamide (NAM). Finally, BG supplementation promotes the growth of *L. johnsonii* and *B. uniformis*, and the production of ILA was confirmed in healthy individuals. These findings shed light on the phenomenon of bacterial cross-feeding and elucidate the intricate interplay between bioactive dietary compounds, gut microbiota, and host health.

Methods

Preparation of BG

BG (linked via (1 → 3) and (1 → 4) linkages, purity > 90%) was obtained from barley (Haidong, Qinghai Province, China) as described in our previous work [16]. In brief, dehulled barley was powdered and immersed in 85% ethanol (1:10, w/v) for 3 h to remove impurities. After drying, the powder was extracted with distilled water (1:10, w/v) at 52 °C for 2 h, followed by thermostable α-amylase treatment (1.5%, v/v) at 95 °C for 3 h and porcine pancreatin treatment (0.5%, w/v) at 40 °C for 3 h. The mixture was filtered through cheesecloth, and the supernatant was collected and then precipitated with 95% ethanol (1:4, v/v). The collected residues were redissolved in distilled water and subjected to dialysis and lyophilization to obtain barley BG.

Animal experiments

Male C57BL/6J mice (5 weeks old) were purchased from Charles River (Beijing, China). All mice were housed under specific pathogen-free (SPF) conditions with a 12-h light–dark cycle and provided with standard chow and water ad libitum and were acclimatized for 1 week before any treatment. Mice were randomly assigned to the control group and intervention group.

For the BG efficiency assay in colitic mice, mice were treated with 400 mg/kg [17] of BG by daily gavage for 14 days, and 3% (w/v) dextran sulfate sodium (DSS) (molecular weight: 36,000–50,000, MP Biochemical) was added to the drinking water from day 7 to day 14. The vehicle group was given an equivalent volume of PBS by gavage.

For the *L. johnsonii* efficiency assay in colitic mice, mice were treated with 1×10^8 CFU of *L. johnsonii*, heat-killed *L. johnsonii*, or *L. johnsonii* ATCC 33200 in 100 μL of sterile anaerobic PBS by daily gavage for 14 days, and 3% (w/v) DSS was added to the drinking water from day 7 to day 14. The vehicle group was given an equivalent volume of sterile anaerobic PBS by gavage.

For the *L. johnsonii* colonization efficiency and ILA production in vivo, germ-free (GF) mice and SPF mice were orally gavaged with 1×10^8 CFU of *L. johnsonii* or an equal volume of PBS for 1 week. Fecal samples were collected after 1 week of intervention.

For the ILA efficiency assay in colitic mice, ILA was dissolved in DMSO to make a stock solution and diluted in PBS immediately before use. Mice were treated with 20 mg/kg [18] of ILA by daily gavage for 14 days, and 3% (w/v) DSS was added to the drinking water from day 7 to day 14. The vehicle group was given an equivalent volume of diluted DMSO by gavage.

For the treatment with AhR antagonist CH223191, mice were treated with 10 mg/kg of CH223191 which was dissolved in 0.5% sodium carboxymethyl cellulose by daily gavage for 14 days. The vehicle group was given an equivalent volume of 0.5% sodium carboxymethyl cellulose by gavage.

For the treatment with NAM, mice were treated with 100 mg/kg [19] of NAM by daily gavage for 14 days, and 3% (w/v) DSS was added to the drinking water from day 7 to day 14. The vehicle group was given an equivalent volume of PBS by gavage.

In assays with *B. uniformis* and NAM-synthesis-deficient *B. uniformis*, mice were treated with 1×10^8 CFU of *B. uniformis* and NAM-synthesis-deficient *B. uniformis* in 100 μL of sterile anaerobic PBS by daily gavage for 14 days, and 3% (w/v) DSS was added to the drinking water from day 7 to day 14. The vehicle group was given an equivalent volume of sterile anaerobic PBS by gavage.

Mice were monitored daily at the same time for body weight loss, the severity of diarrhea, and rectal bleeding during the period of DSS treatment. Weight loss was calculated relative to starting weight before giving DSS of the same mouse and was scored as follows: 0, less than 1%; 1, 1–6%; 2, 6–12%, 3, 12–18%; and 4, more than 18%. Diarrhea was scored as follows: 0, normal; 1, soft but still formed; 2, soft; 3, very soft and wet; and 4, watery diarrhea. Blood in stools was scored as follows: 0, normal; 1, brown color; 2, reddish color; 3, blood traces in stool visible; and 4, gross rectal bleeding. The disease activity index (DAI) was the mean of the total score of the three parameters [20].

Antibiotic treatment

For intestinal microbiota depletion, mice were treated with antibiotic cocktails (ampicillin, 100 mg/kg; metronidazole, 100 mg/kg; vancomycin, 50 mg/kg; neomycin, 100 mg/kg) by daily gavage for 7 days [21].

Fecal microbiota transplantation

The microbiota donor mice were treated with 400 mg/kg/day of BG or PBS for 7 days, followed by a daily collection of feces. Feces from each group were pooled and transferred to an anaerobic chamber. Approximately, 100 mg of feces was resuspended in 1 mL of sterile anaerobic PBS, and the impurity was removed by centrifugation at 800 × g, 4 °C for 3 min. The bacteria pellets were collected by centrifugation at 8000 × g, 4 °C for 10 min, and resuspended in 1 mL of sterile anaerobic PBS. The recipient mice were pre-treated with an antibiotics cocktail as mentioned above, followed by daily oral gavage of 200 μL suspension for 7 days. After the seventh FMT, the mice were treated with 3% (w/v) DSS for 7 days.

16S rRNA gene sequencing and data analysis

Total DNA was extracted from stool samples or fecal culture samples using a Tiangen stool DNA extraction kit. The V4 region of the 16S rRNA gene was amplified by PCR from the extracted and purified genomic DNA using 515 forward and 806 reverse primer pairs. PCR amplification was performed on a PCR System (Bio-Rad, Hercules, CA, USA), and the PCR amplification products were separately extracted from a 2% agarose gel and further purified using a Tiangen agarose gel DNA purification kit. The purified amplicons were quantified using a Qubit Fluorometer (Thermo Fisher Scientific, Waltham, MA, USA), pooled in equimolar, and sequenced on an Illumina MiSeq platform (Illumina, San Diego, CA, USA).

Raw sequencing data were processed with QIIME2 (version 2020.11) [22]. In brief, the forward and reverse reads each were truncated at 200 bases. Paired-end reads were merged, trimmed, filtered (the feature with a sum frequency of less than 10 at each group and the feature that appeared in less than 3 samples were discarded), aligned, and clustered by amplicon sequence variants (ASVs) using DADA2 [23]. Taxonomy was assigned using the Greengenes reference (version 13.8) database [24]. Analysis of alpha diversity (one-way ANOVA followed by Tukey's post hoc test), beta diversity (weighted UniFrac distance followed by ANOSIM test), and bacterial taxonomic distributions were performed using MicrobiomeAnalyst (version 2.0) [25]. Linear discriminant analysis effect size (LEfSe) analysis was performed by Galaxy to identify the major bacteria taxa enriched in different groups, and the effect size of the differentially abundant taxa was obtained through linear discriminant analysis (LDA) based on the Kruskal–Wallis test at an α setting of 0.05 [26]. The indicator species analysis was performed using the R software (version 4.0.4) by package indicspecies (version 1.7.6) [27] to identify key associations between species and groups.

RNA extraction and RNA-seq

The total RNA of colonic tissues was extracted with TRIzol reagent (Thermo Fisher Scientific). The quantity and quality of RNA were examined with a NanoDrop ND-1000 spectrophotometer (Thermo Scientific, Waltham, MA, USA) and Agilent 2100 bioanalyzer (Agilent Technologies, USA). Libraries were constructed using the NEBNext Ultra RNA Library Prep Kit for Illumina according to the manufacturer's instructions and then sequenced on the Illumina NovaSeq 6000 (Illumina, San Diego, CA, USA). Reads were aligned to the reference genome using HISAT2 (version 2.0.5) [28]. Differential expression analysis was performed using the DESeq2 R package (version 1.20.0) [29]. Genes with a

P-value < 0.05 and fold change > 1.5 were selected as differentially expressed genes (DEGs).

Gene expression analysis

Reverse transcription of total RNA was performed using the PrimeScript RT reagent kit (Takara). Quantitative real-time PCR (RT-qPCR) was performed using TB Green Premix Ex Taq II (Takara) on a QuantStudio 7 Flex Real-Time PCR system (Thermo Fisher Scientific, Waltham, MA, USA). The primers are listed in the Table S1. β-actin was used as an endogenous control. The relative mRNA expression levels were calculated using the $2^{-\triangle\triangle Ct}$ quantification method.

Non-targeted metabolomics

The metabolites of colonic contents and bacteria culture supernatant were extracted according to the previously described method [30], with a slight modification. Briefly, colonic contents (50 mg) were mixed with 400 μL ice-cold 80% methanol (v/v) and homogenized using a KZ-II homogenizer (Servicebio, Wuhan, China). For bacterial culture supernatant, 200 μL supernatant was mixed with 200 μL ice-cold methanol and vortexed for 1 min. Then, all samples were sonicated in an ice water bath for 20 min and centrifuged at 18,000 rpm, 4 °C for 20 min. The supernatants were collected and analyzed using a Shimadzu Nexera X2 UPLC system (Kyoto, Japan) coupled with an AB SCIEX TripleTOF 5600 mass spectrometer [31]. Chromatographic separation was carried out at 40 °C with an ACQUITY UPLC HSS T3 column (2.1 mm × 100 mm, 1.8 μm). The acquired row mass data were processed using Progenesis QI software (version 2.0, Waters). Metabolite annotation was made by searching MS and MS/MS information against the HMDB database (version 4.0) and METLIN (version 1.0.6499.51447).

Targeted quantification of indole derivatives and NAM

Feces, colonic contents, or bacteria culture supernatant were mixed with extraction solvent (mentioned above) containing 1 μM chlorpropamide (internal standard). Extraction methods were consistent with those described in "non-targeted metabolomics." Analysis of indole derivatives and NAM was performed by the liquid chromatography-tandem mass spectrometry (LC–MS/MS) system composed of a Shimadzu Nexera X2 high-performance liquid chromatography system (Kyoto, Japan) coupled to a SCIEX 4500 triple quadrupole linear ion trap mass spectrometer (AB SCIEX, Framingham, MA, USA). Chromatographic separation was employed with an ACQUITY UPLC HSS T3 column (2.1 mm × 100 mm, 1.8 μm), and mobile phase A contained 0.1% FA in water and mobile phase B 0.1% FA in acetonitrile. All analytes were detected in positive ion multiple reaction monitoring (MRM) modes. Chromatographic separation was performed using a linear gradient as follows: 0–4 min, 5–40% B; 4–6 min, 40–80% B; 6–8 min, 80% B; and 8–10 min, 80–5% B. Operational control of the LC–MS/MS was performed with Analyst (version 1.6.2), and quantitative analysis was performed using MultiQuant software (version 3.0.1).

Generation of the *cobB*-deficient strain of *B. uniformis*

A CRISPR/Cas-based genome editing system was used to edit genes in *B. uniformis* [32]. Briefly, linear tool plasmid, sgRNA, and homologous arms (800 bp repair templates) were obtained through PCR and cloned by cloning kit to afford the *cobB* disruption plasmid. The *cobB* disruption plasmid was introduced into *B. uniformis* via *E. coli-Bacteroides* conjugation. The transconjugants were selected on gentamicin and erythromycin after 24–48 h anaerobic incubation at 37 °C. Then one chosen clone was incubated overnight at 37 °C in GAM medium with gentamicin and erythromycin under anaerobic conditions. Then the overnight cultures were diluted 1:100 in GAM medium with aTc induced for gene edit (aTc final concentration 100 ng/mL) and further cultured at 37 °C for 24 h. Finally, plate streaking was used to pick up colonies of *cobB* disruption strains which were verified by PCR and sequencing.

Microbial strains

L. johnsonii NSP009 (GuangDong Microbial Culture Collection Center, number: GDMCC63248), *L. plantarum*, *L. murinus*, *L. reuteri*, *L. fermentum*, *L. rhamnosus*, *L. gasseri*, *L. paracasei*, *L. casei*, and *L. salivarius* were isolated from mouse colonic contents, and *L. johnsonii* NSP009 was used for mechanism study. *L. johnsonii* ATCC33200 was purchased from the American Type Culture Collection (ATCC; Manassas, VA, USA). *B. uniformis* was isolated from the feces of healthy humans. All microbes used in this study were cultured in an anaerobic chamber (Coy) with an atmosphere of 5% hydrogen, 5% carbon dioxide, and 90% nitrogen at 37 °C. For the growth of *L. johnsonii*, a media of Man-Rogosa-Sharpe (MRS) with L-cysteine HCl (0.5 g/L) was used. For the growth of *B. uniformis*, a media of brain heart infusion (BHI) with L-cysteine HCl (0.5 g/L), vitamin K1 (10 mg/L), hemin (5 mg/L), and resazurin (1 mg/L) was used. The purity of the cultures was monitored by plating serial dilutions. All media, buffer, glass, and plasticware used in the study were exposed to the anaerobic conditions at least 12 h before use.

In vitro growth assays

For in vitro fermentation assays, mouse colonic contents were collected and cultured in a specific medium

as described [33]. Briefly, the medium contained minerals, bile salts, cysteine, hemin, and peptone. The vitamin solution and BG solution were added from stock solutions after autoclaving of the medium, directly before inoculation with the bacterial suspension. All samples were incubated in a Coy anaerobic chamber at 37 °C for 24 h.

For *Lactobacillus* isolation and identification, the fermented samples were serially diluted in sterile PBS and spread onto MRS agar plates. After incubation under anaerobic conditions at 37 °C for 72 h, the colonies were picked, subcultured, and amplified by PCR using 27 forward and 1492 reverse primer pairs. Bacterial isolates were identified using 16S rRNA gene sequencing.

For *B. uniformis* isolation and identification, 10 mg human feces samples were homogenized in 1 mL sterile anaerobic PBS and serially diluted in sterile PBS. The diluted samples were spread onto modified BHI agar medium [BHI supplemented with vancomycin (7.5 mg/L), kanamycin (100 mg/L), L-cysteine HCl (0.5 g/L), vitamin K1 (10 mg/L), hemin (5 mg/L), and resazurin (1 mg/L)] and cultured anaerobically at 37 °C for 48 h to obtain *B. uniformis*. Bacterial isolates were identified using 16S rRNA gene sequencing.

For cross-feeding assays, *B. uniformis* were grown overnight in BHI medium [supplemented with L-cysteine HCl (0.5 g/L), vitamin K1 (10 mg/L), hemin (5 mg/L), and resazurin (1 mg/L)] at 37 °C under anaerobic conditions, and 1% (v/v) of the BHI precultures was inoculated in the basal medium [proteose peptone, 10 g/L; beef extract, 10 g/L; yeast extract, 5 g/L; Tween 80, 1 mL/L; ammonium citrate trihydrate, 2 g/L; sodium acetate trihydrate, 5 g/L; magnesium sulfate, 0.1 g/L; manganese sulfate, 0.05 g/L; dipotassium phosphate, 2 g/L; L-cysteine HCl, 1 g/L; and resazurin (1 mg/L)] [34] containing BG (5 g/L) or glucose (5 g/L) as the sole carbon source, respectively. *L. johnsonii* was grown overnight in MRS medium supplemented with L-cysteine HCl (0.5 g/L) at 37 °C under anaerobic conditions, and 1% (v/v) of the MRS precultures was inoculated in basal medium containing BG (5 g/L) or glucose (5 g/L) as the sole carbon source, respectively.

The content of total carbohydrates was determined according to the previously described [35, 36], with a slight modification. Briefly, 10 μL cell-free supernatants obtained through centrifugation at 8000 × g for 15 min at 4 °C were added with 500 μL of ultrapure water, 500 μL of phenol, and 2 mL of sulfuric acid and then reacted at room temperature for 30 min. The absorbance value of the reaction mixture was determined at 490 nm using a SpectraMax 190 Microplate Reader (Molecular Devices Inc.).

The content of oligosaccharides was measured according to previously described methods [37, 38], with a slight modification. Briefly, 300 μL cell-free supernatants obtained through centrifugation at 8000 × g, 4 °C for 15 min, were added with ultrapure water to 800 μL and then were deproteinized using Carrez A (100 μL) and Carrez B (100 μL) reagents. The above solution was diluted by two times and analyzed by HPAEC-PAD. HPAEC-PAD was performed on a Dionex ICS-5000 HPLC system operated by Chromeleon software (version 7.0). Samples were separated on a 3×250 mm Dionex CarboPac PA200 column (Thermo Scientific, Waltham, MA, USA). Solvent A was ultrapure water, solvent B was 1 M sodium hydroxide, and solvent C was 1-M sodium acetate. Conditions used were 0–5 min, 10% B (initial conditions); 5–12 min, 10% B, linear gradient from 0 to 30% C; 12.0–12.1 min, linear gradient from 10–50% B, linear gradient from 30 to 50% C; 12.1–13.0 min, the exponential gradient of B and C back to initial conditions; and 13–17 min, initial conditions. A mixture of glucose, G3G, G4G3G, and G4G4G3G was used as a standard.

To determine NAM production by *B. uniformis* in vitro, the *B. uniformis* were grown overnight in BHI medium [supplemented with L-cysteine HCl (0.5 g/L), vitamin K1 (10 mg/L), hemin (5 mg/L), and resazurin (1 mg/L)] at 37 °C under anaerobic conditions, washed twice in PBS (containing 0.5 g/L L-cysteine HCl), and resuspended in PBS at a 1:1dilution at 37 °C for 48 h. The samples were collected at the indicated time points, and the NAM level was analyzed by LC-MS/MS.

To measure NAM utilization by *L. johnsonii* in vitro, the *L. johnsonii* was grown overnight in MRS medium supplemented with L-cysteine HCl (0.5 g/L) at 37 °C under anaerobic conditions, washed twice in PBS (containing 0.5 g/L L-cysteine HCl), and resuspended in PBS (containing 10 μM NAM and 0.5 g/L L-cysteine HCl) at a 1:1dilution at 37 °C for 24 h. The samples were collected at the indicated time points, and the NAM level was analyzed by LC-MS/MS.

To test the ability of metabolites (NAM, N2,N2-dimethylguanosine, and 2′-O-methyladenosine) to promote the proliferation of *L. johnsonii*, the *L. johnsonii* was grown overnight in an MRS medium supplemented with L-cysteine HCl (0.5 g/L) at 37 °C under anaerobic conditions, and washed twice in PBS, followed by inoculation into MRS medium (diluted 10 times) and growth for 32 h. The effect of the metabolites on *L. johnsonii* growth kinetics was analyzed using a SpectraMax 190 Microplate Reader (Molecular Devices Inc.) by measuring the optical density at 600 nm (OD600). For metabolomic analysis and assessment of ILA production by *L. johnsonii* in vitro, the *L. johnsonii* and *L. johnsonii* ATCC33200 were propagated routinely in MRS broth medium with L-cysteine HCl (0.5 g/L) at 37 °C for 48 h. The samples

were collected at the indicated time points, and the ILA level was analyzed by LC-MS/MS.

Quantification of bacteria

Fecal DNA was extracted using the Tiangen stool DNA extraction kit according to the manufacturer's instructions. The primers listed in Table S2 were used for PCR-based amplification. RT-qPCR was performed using TB Green Premix Ex Taq II (Takara) on a QuantStudio 7 Flex Real-Time PCR system (Thermo Fisher Scientific, Waltham, MA, USA). The PCR conditions included 50 °C for 2 min and then 95 °C for 30 s, followed by 40 cycles of denaturation at 95 °C for 20 s, annealing at 56 °C for 30 s, and extension at 72 °C for 30 s. Standard curves were constructed with reference bacteria as described previously [39].

Histopathological and immunohistochemical analysis

Collected colon samples were fixed in 4% paraformaldehyde. Paraffin-embedded sections were cut at a thickness of 4 μm and stained with hematoxylin and eosin (H&E) and Alcian-blue/periodic acid-Schiff (AB/PAS). Whole

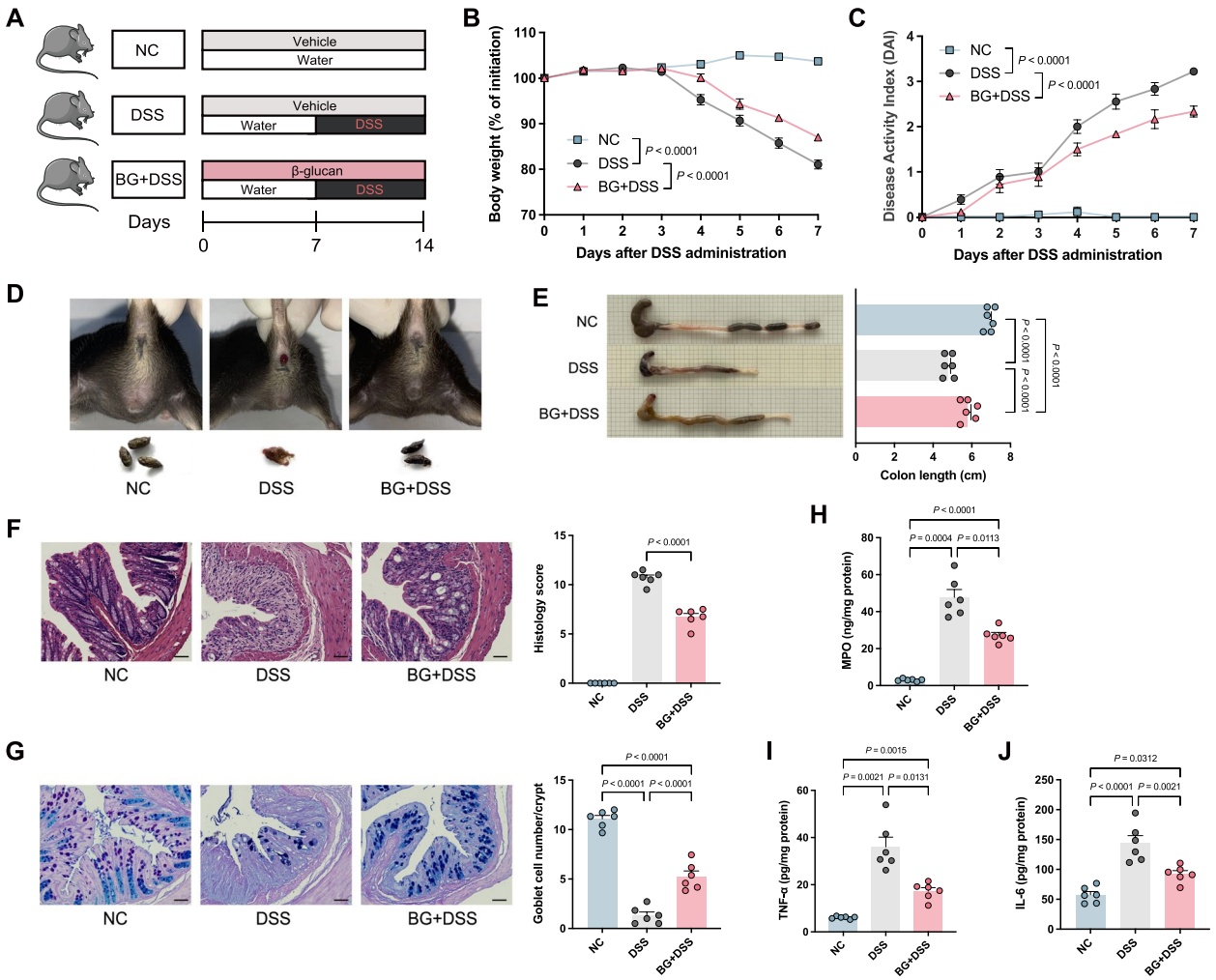

Fig. 1 BG ameliorates colitis symptoms. **A** Experimental schema for **B**–**J**. Mice were treated with 400 mg/kg BG or PBS by daily gavage for 14 days and treated or not with 3% (w/v) DSS from day 7 to day 14. **B**, **C** Body weight (**B**) and disease activity index (**C**) were monitored daily after DSS treatment. **D** Representative photographs of diarrhea and rectal bleeding from each group. **E** Representative photographs (left) and length quantification (right) of colon tissues. **F** Representative H&E-stained sections (left) and histology score (right) of the distal colon. Scale bars, 50 μm. **G** Representative AB/PAS-stained sections (left) and the number of goblet cells per crypt (right). Scale bars, 50 μm. **H**–**J** Colonic levels of MPO (**H**), TNF-α (**I**), and IL-6 (**J**). Data are presented as the mean ± SEM. $n = 6$ mice per group. Statistical analysis was performed using two-way ANOVA followed by Tukey's post hoc test for **B** and **C**; one-way ANOVA followed by Tukey's post hoc test for **E**, **G**, and **J**; *t*-test for **F** which compared only the DSS group with the BG + DSS group; and one-way ANOVA followed by Dunnett's post hoc tests for **H** and **I**. BG, *β*-glucan; H&E, hematoxylin and eosin; AB/PAS, Alcian Blue/periodic acid-Schiff. MPO, myeloperoxidase

cross sections were scanned and imaged in a digital pathology system (Leica Aperio LV1). For H&E staining, histological pathology was scored according to previous studies [40, 41]: epithelium damage (0–4 scale), the severity of inflammation (0–4 scale), and depth of lesion (0–4 scale). The total histology score was the sum of the three parameters. For AB/PAS staining, the number of goblet cells was observed and counted in at least 20 randomly selected crypts per section. Only crypts that were cut longitudinally from the crypt opening to the bottom of the crypt were considered. For immunohistochemistry (IHC), paraffin sections were incubated with antibodies specific to Muc2. The percentage of the positive area was calculated by the ImageJ (version 1.53 k) software.

Cytokine quantification

Colonic tissues were homogenized in PBS, and supernatants were collected by centrifugation at 10,000 rpm, 4 °C for 10 min for cytokine analysis. Cytokine levels were determined by enzyme-linked immunosorbent assay (ELISA) kit according to the manufacturer's instructions (Fcmacs). Protein levels were normalized to the total protein concentration determined by a BCA assay (Beyotime).

Human study

Thirty healthy participants were recruited in the First Affiliated Hospital of Nanchang University and Nanchang University (Nanchang, China) and provided informed consent. The primary inclusion criteria included healthy males and females aged 18 to 55 years who had not received antibiotics in the 3 months before the start of the study. Exclusion criteria included the following: (1) use of antibiotics, probiotic, or prebiotic supplements for 3 months before the start of the study, (2) patient history of GI diseases or surgeries, (3) smoking, (4) alcohol intake five times/week, and (5) allergy to gluten. A total of 30 participants (an average age of 25.4 ± 1.9 years), including 15 males and 15 females, were used for the final analysis.

All participants were provided an oats powder (Lantmännen) containing 5 g of BG (linked via (1 → 3) and (1 → 4) linkages) daily for 2 weeks. Participants were instructed to dissolve the powder in warm water and consume the supplement as part of their regular dietary intake. Stool samples were collected at baseline and 14 days after BG supplementation using a stool collection device (BioRise, LF005). After collection, stool samples were snap frozen in dry ice and stored at − 80 °C until analysis.

Statistical analysis

All statistical analyses were performed using GraphPad Prism (version 10.1.0) and SPSS (version 26.0). The data are presented as the mean ± standard error of the mean (SEM). The sample sizes for human participants were determined using GraphPad StatMate (version 2.0). As for animal experiments and in vivo studies, sample sizes were not statistically predetermined but were similar to those reported in previously published works [42]. No data were excluded during the data analysis. Parametric or nonparametric statistical tests were applied appropriately after testing for the normal distribution of data. For comparison between two groups, an unpaired *t*-test (with equal variances) or unpaired *t*-test with Welch's correction (with different variances) was used when samples were normally distributed, and the Mann–Whitney *U*-test was used when samples were not normally distributed. For comparisons among more than two groups, one-way ANOVA followed by Tukey's (with equal variances) or Dunnett's (with different variances) post hoc test was used when samples were normally distributed, and Kruskal–Wallis was used when samples were not normally distributed. Two-way ANOVA followed by Tukey's or Bonferroni's post hoc test was used if needed. *P*-values < 0.05 were considered statistically significant. When applicable, the *P*-value is adjusted by the Benjamini–Hochberg procedure to control the false discovery rate (FDR) < 0.05.

(See figure on next page.)

Fig. 2 BG promotes the growth of *L. johnsonii*. **A**–**F** Bacterial DNA was extracted from the feces of mice on day 14 and analyzed by 16S rRNA gene sequencing. *n* = 6 mice per group. **A** Alpha diversity, evaluated by Chao1 and Shannon index. Data are presented as the mean ± SEM. Statistical analysis was performed using one-way ANOVA followed by Tukey's post hoc test. **B** Principal coordinate analysis (PCoA) plot based on the unweighted UniFrac metric. **C** Relative abundance at the genus level. **D** Comparison of relative abundance of bacteria between DSS and BG + DSS group was calculated by linear discriminant analysis effect size (LEfSe). Taxa meeting an LDA score threshold > 2.0 is shown. **E** The OTUs associated with each group were identified by indicator analysis. The heat map shows the relative abundance and indicator values of indicator OTUs with a cutoff of FDR-adjusted *P* < 0.05 and indicator value > 0.8. OTU identifier (ID) and taxonomy of the indicators are shown on the right. Unc., unclassified. **F** Heatmap of the correlation between bacteria and colitis-related parameters. Spearman's rank test: **Q* < 0.05, ***Q* < 0.01, Q value (FDR-adjusted *P*-value). **G**–**J** Bacterial DNA was extracted from fermented samples. *n* = 3 per group. **G** The schematic diagram for in vitro fermentation. **H** Relative abundance at the genus level. **I** Comparison of relative abundance of bacteria between 0 and 24 h in the fermented sample by LEfSe. **J** Schematic diagram and results of *Lactobacillus* screening and identification

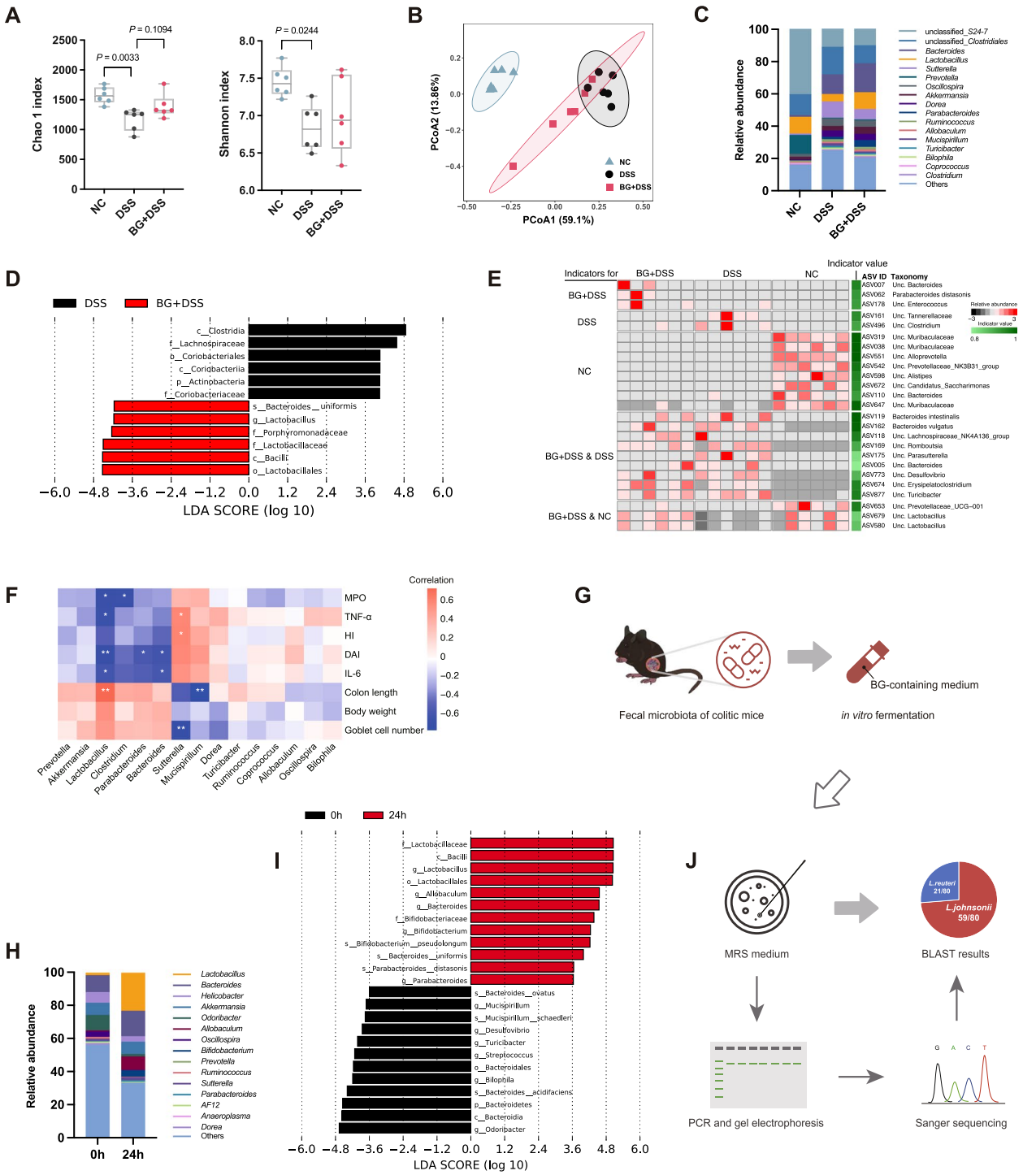

Fig. 2 (See legend on previous page.)

Results

BG alleviates DSS-induced colitis

To investigate the effect of BG on colitis, mice were pre-treated with BG by oral gavage daily for 7 days, with 3.0% (w/v) DSS and BG for further 7 days (Fig. 1A). During the colitis induction, BG supplementation significantly reduced body weight loss and alleviated pronounced diarrhea and rectal bleeding, along with colon shortening (Fig. 1B–E). Moreover, histological assessments of mouse colons indicated that BG effectively reduced

intestinal epithelial destruction and limited inflammatory cell infiltration (Fig. 1F). AB/PAS staining displayed a reduced goblet cell loss in the BG + DSS group compared to the DSS group (Fig. 1G). Myeloperoxidase (MPO) and inflammatory cytokine (including TNF-α and IL-6) levels were significantly reduced in the BG + DSS group of mice compared to the DSS group (Fig. 1H–J). Taken together, these data suggested that BG could protect against DSS-induced colitis in mice.

BG alters the composition of gut microbiota in colitic mice

Ulcerative colitis is typically associated with dysbiosis of gut microbiota [6]. DSS treatment significantly reduced species richness, and supplementation of BG tended to reverse this reduction (Chao1 index, $P = 0.1094$, Fig. 2A). BG also altered the gut microbiota composition in mice (Fig. 2B). Similar to previous studies, we observed an increased abundance of taxa belonging to Proteobacteria and a decreased abundance of Bacteroidetes in colitic mice (Fig. S1A) [43]. The relative abundance of *Lactobacillus* and *Prevotella* was substantially decreased in DSS-treated mice at the genus level compared to normal mice. BG significantly increased the abundance of *Lactobacillus*, *Bacteroides*, and *Parabacteroides* and reduced the abundance of *Sutterella* and *Mucispirillum* (Fig. 2C). Based on the results of the LEfSe, we noted a significant increase in the abundance of Lactobacillaceae, *Lactobacillus*, and *Bacteroidetes uniformis* and a significant decrease in Coriobacteriaceae and Lachnospiraceae in BG-treated mice (Fig. 2D, Figure S1B). In addition, indicator species analysis showed that ASV679 and ASV580 which were assigned to *Lactobacillus* decreased in the DSS group but increased in the BG + DSS group (Fig. 2E). A Spearman rank correlation analysis further demonstrated that the abundance of *Lactobacillus* was positively correlated with colon length and negatively correlated with the levels of MPO, TNF-α, IL-6, and DAI (Fig. 2F, Fig. S1C). These data suggested that the increased *Lactobacillus* induced by BG treatment may contribute to colitis mitigation

Alleviation of colitis by BG is microbiota dependent

To investigate the essential role of the gut microbiota in the amelioration of colitis by BG, we depleted the endogenous microbial community in mice through antibiotic (Fig. S2A). This depletion was further confirmed by RT-qPCR and plate counting techniques (Fig. S2B). Subsequently, mice were orally gavaged with either BG or vehicle, followed by DSS-induced colitis treatment. It was found that there were no significant differences observed between the DSS-ABX group and the BG-ABX group in terms of weight loss, colon length reduction, histological scores, and goblet cell numbers (Fig. S2C–H). These findings indicate that the gut microbiota is necessary for the preventive effects of BG on colitis. Furthermore, the outcomes of fecal microbiota transplantation (FMT) revealed that the microbiota modulated by BG exhibited beneficial effects in recipient mice to withstand DSS-induced weight loss, diarrhea, rectal bleeding, epithelial injury, and preservation of colon length and goblet cell numbers (Fig. S3A–F). Together, these data provide cohesive evidence that the alleviation of colitis by BG is microbiota dependent.

(See figure on next page.)

Fig. 3 *L. johnsonii* protects against colitis and activates the AhR signaling pathway. **A** Experimental schema for **B**–**P**. Mice were treated with 1×10^8 CFU of *L. johnsonii*, heat-killed *L. johnsonii*, or *L. johnsonii* ATCC 33200 in 100 µL of sterile anaerobic PBS by daily gavage for 14 days, and 3% (w/v) DSS was added to the drinking water from day 7 to day 14. **B** The abundance of *L. johnsonii* in the feces of mice. **C**, **D** Body weight (**C**) and disease activity index (**D**) were monitored daily after DSS treatment. **E** Representative photographs (left) and length quantification (right) of colon tissues. **F** Colonic levels of MPO, IL-6, and TNF-α. **G** Representative H&E-stained sections (upper) and AB/PAS-stained sections (lower) of the distal colon. Scale bars, 50 µm. **H** Histology scores were determined from H&E-stained sections. **I** The number of goblet cells per crypt was determined from AB/PAS-stained sections. **J**–**M** Transcriptomic changes in the colon were regulated by *L. johnsonii*. $n = 3$ mice per group. **J** Principal component analysis (PCA) of transcriptional profiling. **K** Volcano plot of differentially expressed genes induced by *L. johnsonii*. **L** Heatmap of reported AhR target mediators and IL-22-related barriers regulating genes. **M** Correlation network of colitis-related parameters and AhR-related genes as in Fig. 3L. Purple nodes indicate colitis-related parameters; orange nodes indicate genes. Only nodes with FDR-adjusted $P < 0.1$ were shown. The edges are colored based on the positive or negative Spearman correlation coefficients, with orange indicating a positive correlation and purple a negative correlation, and the stronger the correlation, the thicker the edge. **N**–**P** Colon tissues were harvested from PBS- or *L. johnsonii*-treated mice. **Q**–**T** Colon tissues were harvested from PBS- or BG-treated mice. Related to Fig. 1. **N**, **Q** Relative gene expression of AhR-related genes in colon tissue assessed by RT-qPCR. **R** Relative gene expression of pattern recognition receptors involved in recognizing fungal-derived BG in colon tissue assessed by RT-qPCR. **O**, **S** Colonic levels of IL-22. **P**, **T** Representative Muc2-stained colon sections (left) and quantified Muc2-positive area (right). Scale bars, 50 µm. Data are presented as the mean ± SEM. $n = 6$ mice per group if not specifically mentioned. Statistical analysis was performed using one-way ANOVA followed by Dunnett's post hoc tests for **B**, **H** and **I**, two-way ANOVA followed by Tukey's post hoc test for **C** and **D**, one-way ANOVA followed by Tukey's post hoc test for **E** and **F**, and *t*-test or *t*-test with Welch's correction for **N**–**T**. *LJ*, *L. johnsonii*; HK-*LJ*, heat-killed *L. johnsonii*; *LJ*-ATCC, *L. johnsonii* ATCC 33200; H&E, hematoxylin and eosin; AB/PAS, Alcian Blue/periodic acid-Schiff; MPO, myeloperoxidase; HI, histological index

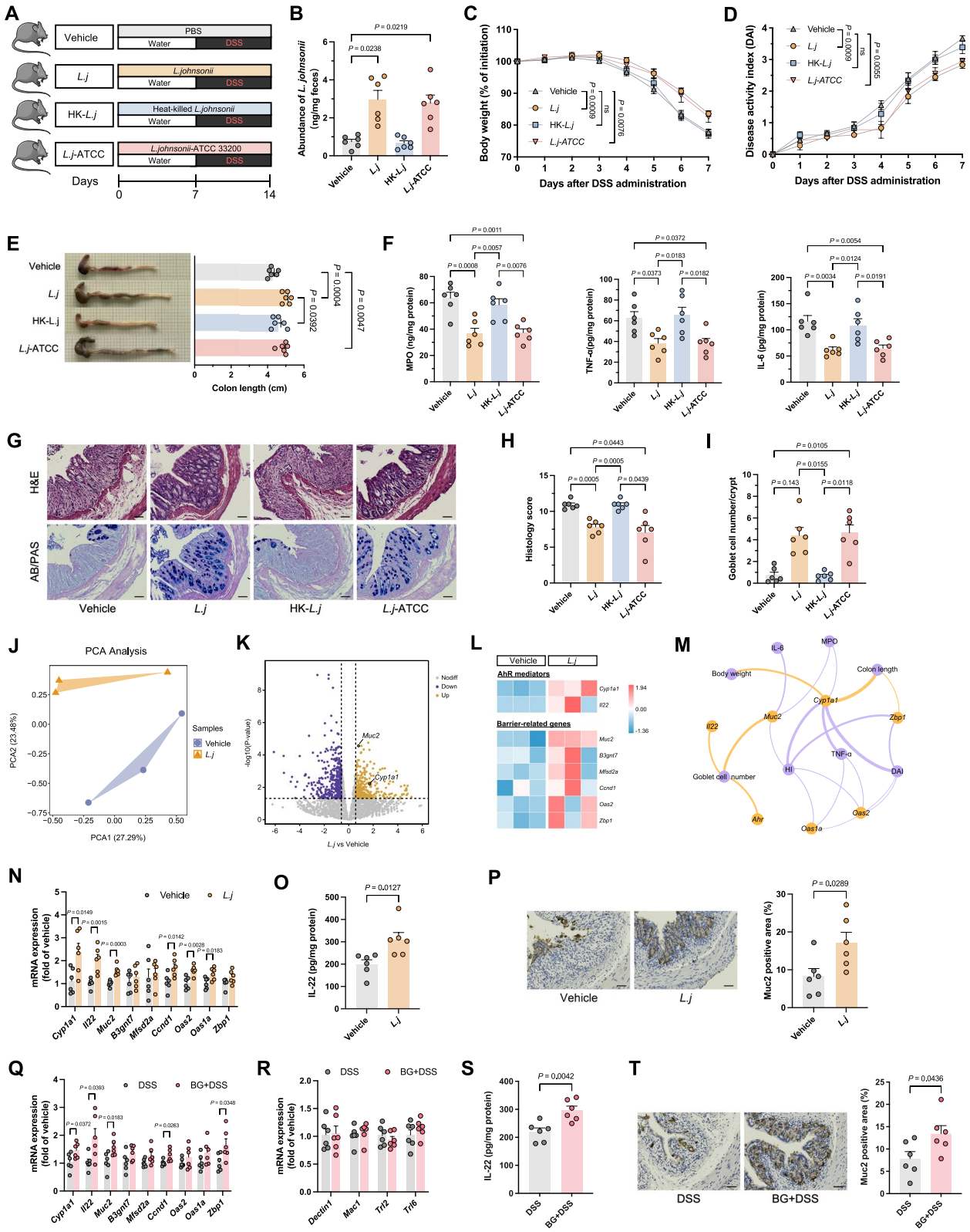

Fig. 3 (See legend on previous page.)

L. johnsonii is the primary *Lactobacillus* promoted by BG

To identify the specific *Lactobacillus* strains enriched by BG within the colitis microbial community, we conducted an in vitro fermentation experiment using fecal microbiota from colitic mice, with BG serving as the sole carbon source in the culture medium (Fig. 2G). By measuring the changes in total carbohydrate content, it was observed that BG was primarily consumed within the initial 24 h of fermentation (Fig. S4A). Similarly, BG primarily promoted the proliferation of *Lactobacillus* in vitro, along with an increase of *Bacteroides* (especially *B. uniformis*), *Bifidobacterium*, and *Parabacteroides* (Fig. 2H, I). Subsequently, selective isolation of *Lactobacillus* species was performed from the 24-h fermented samples using MRS agar (Fig. 2J), and individual colonies were identified through 16S rRNA sequencing. A total of 80 cultivable *Lactobacillus* colonies were obtained, including 59 *L. johnsonii* and 21 *L. reuteri* strains (Fig. 2J). Upon further quantification of these two *Lactobacillus* species in colitic mice and fermented samples, a significant increase in the abundance of *L. johnsonii* was observed (Fig. S4B, C). Furthermore, when normal SPF mice were subjected to 1 week of BG intervention, a similar increase in *L. johnsonii* was observed (Fig. S4D). Remarkably, this phenomenon was also observed in FMT recipient mice (Fig. S4E, F). These results suggest that BG has a growth-promoting effect on *L. johnsonii* which may be the key functional bacterium.

L. johnsonii protects against colitis and activates the AhR signaling pathway

Since the growth-promoting effect of BG on *L. johnsonii* was confirmed both in vitro and in vivo, further investigation was conducted to examine the impact of *L. johnsonii* on DSS-induced colitis (Fig. 3A). Oral administration of *L. johnsonii* substantially enhanced its abundance in the mice feces, while heat-killed *L. johnsonii* had little effect (Fig. 3B).

Compared to the vehicle group, both *L. johnsonii* and the standard strain of *L. johnsonii* (*L. j*-ATCC) administration ameliorated DSS-induced colitis, evidenced by reduced weight loss, DAI score, and colonic shortening. However, the same dose of heat-killed *L. johnsonii* (HK-*L. j*) did not improve the colitis-related parameters (Fig. 3C–E). Levels of MPO, TNF-α, and IL-6 were significantly decreased in *L. johnsonii*- and standard strain of *L. johnsonii*-treated mice compared to vehicle and heat-killed *L. johnsonii* group (Fig. 3F). Histological examination showed a significant reduction in colonic inflammation and architectural distortion, with preserved goblet cell number in *L. johnsonii*- and standard strain of *L. johnsonii*-treated mice (Fig. 3G–I). The protective effect was only observed with metabolically active bacteria since heat-killed *L. johnsonii* did not have a mitigation effect.

To better understand how *L. johnsonii* improved barrier function, transcriptional profiling of the colonic

(See figure on next page.)

Fig. 4 *L. johnsonii*-derived ILA alleviates colitis . **A**, **B** Mice were treated with PBS or *L. johnsonii* as in Fig. 3A. The colonic contents were collected for untargeted metabolomics profiling. **A** Volcano plot of detected metabolites, with differential metabolites identified based on thresholds (dotted lines) of |log2 fold change|> 1 and FDR-adjusted $P < 0.05$. $n = 6$. **B** The MS/MS spectra of the ILA standard (lower) and ILA detected in the sample (upper). **C** Representative extracted ion chromatograms of ILA from cultured *L. johnsonii* and *L. johnsonii* ATCC 33200 compared to medium control at 0 h and 48 h. $n = 3$ per group. **D** The Venn diagram displayed co-altered metabolites among the top 100 significantly altered metabolites in colonic contents from *L. johnsonii*- and BG-treated mice. **E** Correlation network of colitis-related parameters, bacteria, and metabolites from BG-treated mice. Gray nodes indicate colitis-related parameters, blue nodes indicate bacteria, and pink nodes indicate metabolites. Only nodes with FDR-adjusted $P < 0.1$ were shown. The edges are colored based on the positive or negative Spearman correlation coefficients, with pink indicating a positive correlation and blue a negative correlation, and the stronger the correlation, the thicker the edge. **F** The levels of tryptophan and related metabolites in colonic content of PBS- and *L. johnsonii*-treated mice. $n = 3$ per group. **G**–**I** *L. johnsonii* colonization efficiency (**H**) and ILA concentration (**I**) in feces of control- and *LJ*-treated GF mice, as described in the schematic diagram (**G**). $n = 6$ mice per group. **J**–**L** *L. johnsonii* colonization efficiency (**K**) and ILA concentration (**L**) in feces of control- and *LJ*-treated SPF mice, as described in the schematic diagram (**J**). $n = 6$ mice per group. **M** Experimental schema for **N**–**U**. Mice were treated with 20 mg/kg of ILA or PBS daily for 14 days, with or without 10 mg/kg of AhR antagonist CH223191, and 3% (w/v) DSS was added to the drinking water from day 7 to day 14. **N**, **O** Body weight (**N**) and disease activity index (**O**) were monitored daily after DSS treatment. **P** Representative photographs of colon tissues. **Q** The colon length of mice. **R** Representative H&E-stained sections (upper), AB/PAS-stained sections (middle), and immunocytochemistry of Muc2-stained sections (lower) of the distal colon tissue. Scale bars, 50 μm. **S** Histology score (left), the number of goblet cells per crypt (center), and quantified Muc2-positive area (right) of sections. **T** Relative gene expression of *Cyp1a1* and *Il22* in colon tissue assessed by RT-qPCR. **U** Colonic levels of TNF-α, IL-6, and IL-22. Data are presented as the mean ± SEM. $n = 6$ mice per group if not specifically mentioned. Statistical analysis was performed using *t*-test or Mann–Whitney for **F**; Mann–Whitney test for **H** and **I**; *t*-test with Welch's correction for **K** and **L**; two-way ANOVA followed by Tukey's post hoc test for **N** and **O**; one-way ANOVA followed by Tukey's post hoc test for **Q**, **S**, **T** (right), and **U**; and one-way ANOVA followed by Dunnett's post hoc tests for **T** (left). PCA, principal component analysis; VIP, variable importance in projection; TRP, tryptophan; TA, tryptamine; IAM, indole-3-acetamide; IAA, indole-3-acetic acid; IAld, indole-3-carboxaldehyde; IPYA, indole-3-pyruvic acid; ILA, indole-3-lactic acid; IA, 3-indoleacrylic acid; IPA, 3-indolepropionic acid; nd., not detected; GF, germ-free; SPF, specific-pathogen-free

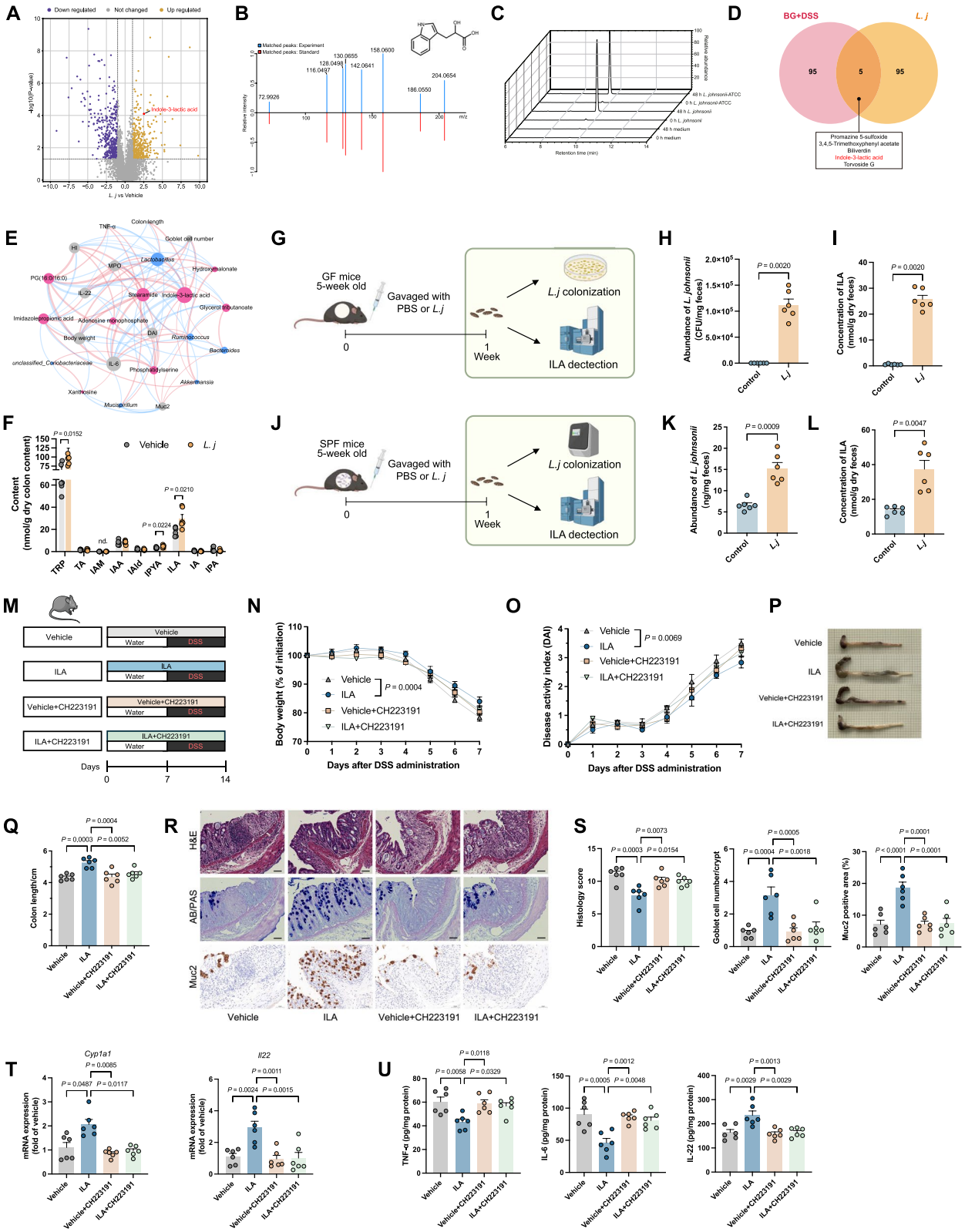

Fig. 4 (See legend on previous page.)

tissue was conducted. The transcriptomic profile was significantly different between the *L. johnsonii* group and the vehicle group (Fig. 3J), with 811 differentially expressed genes identified based on the criteria of fold change (FC) > 1.5 and $P < 0.05$ (Fig. 3K). Among these genes, *Cyp1a1* was significantly upregulated (FC = 3.2815, $P = 0.0064$), which is an important downstream gene of AhR (associated with the negative feedback regulation of AhR). AhR is a transcriptional regulator involved in regulating cytokines that play a role in colitis, including IL-22 and IL-10, which are known to be essential anti-inflammatory cytokines. We found *L. johnsonii* tends to increase the expression of *Il22* (FC = 10.7979, $P = 0.1310$). Similar to the role of IL-22 in regulating the intestinal barrier, *L. johnsonii* intervention upregulated the expression of genes related to mucin production (*Muc2* and *B3gnt7*), epithelial function (*Mfsd2a* and *Ccnd1)*, and antimicrobial defense (*Oas2*, *Oas1a*, and *Zbp1*) in the colon of mice (Fig. 3L). Further, Spearman correlation analysis showed that *Cyp1a1* was positively correlated with body weight and colon length (Fig. 3M) and negatively correlated with DAI, HI, and TNF-α. These findings suggest that *L. johnsonii* may alleviate colitis by enhancing the mucosal barrier through the activation of AhR and IL-22 production.

To validate these findings, the expression of AhR- and barrier-related genes was examined by RT-qPCR, which demonstrated increases in the expression levels of *Cyp1a1* and *Il22*, as well as IL-22-related genes, including *Muc2*, *Ccnd1*, *Oas2*, and *Oas1a* in *L. johnsonii*-treated mice (Fig. 3N). At the protein level, the colonic levels of IL-22 and Muc2 were also significantly increased in mice treated with *L. johnsonii* compared to vehicle (Fig. 3O, P). Additionally, mice treated with BG exhibited elevated *Cyp1a1* and *Il22* gene expression, as well as increased levels of IL-22 and Muc2 in the colon. Since it has been reported that fungal-derived BG activates certain pattern-recognition receptors to regulate inflammation, we examined the expression of relevant genes but did not observe a significant effect (Fig. 3Q–T). The further animal experiment showed that the protective effects of *L. johnsonii* and BG on DSS-induced colitis were abolished when the activation of AhR was inhibited by 2-methyl-2H-pyrazole-3-carboxylic acid (2-methyl-4-*o*-tolylazo-phenyl)-amide (CH223191), indicating that the activation of AhR plays an essential role in the mitigation of colitis by *L. johnsonii* and BG (Fig. S5A–H). Taken together, the activation of the AhR signaling pathway induced by *L. johnsonii* plays a crucial role in alleviating colitis by BG.

L. johnsonii-derived ILA alleviates colitis

Gut microbiota-derived metabolites play a critical role in mediating the intricate interactions between the gut microbiota and the host [44]. The finding that heat-treated *L. johnsonii* did not alleviate colitis led to the hypothesis that metabolites produced by *L. johnsonii* may be necessary to mitigate colitis, with some effective agonist of AhR potentially among them. To identify key metabolites, *L. johnsonii* was cultured in an MRS medium, and non-targeted LC-MS/MS metabolomics was used to identify metabolites in the bacterial culture supernatant. The metabolites in *L. johnsonii* cultured supernatant (LJCS) differed from those in the MRS medium, where key metabolites generated from *L. johnsonii* may drive an anti-inflammatory effect (Fig. S6A, B).

Examination of the metabolic profiles of colonic contents from *L. johnsonii*- and vehicle-treated mice revealed the treatment of *L. johnsonii* induced a specific fecal metabolomic profile (Fig. S6C) and significantly increased the levels of 3-sulfopyruvic acid, choline, pyrocatechol sulfate, L-tryptophan, and ILA (Fig. 4A, Fig. S6D, E). Among them, ILA was previously recognized as an AhR agonist and was also found to be significantly increased in LJCS (Fig. 4B, Fig. S6B) [45]. Additionally, the ability of *L. johnsonii* to produce ILA was confirmed in vitro (Fig. 4C, Fig. S6F), which suggested its potential role in mitigating colitis. Comparison between the metabolic profiles of colon contents from BG- and vehicle-treated mice exhibited significant changes in the metabolites among colitic mice with chenodeoxycholic acid 3-sulfate, hydroxymalonate, ILA, PG (16:0/16:0), and L-tryptophan being the most significantly changed metabolites (Figure S6G–I). A Venn diagram analysis among the top 100 metabolites upregulated by BG and *L. johnsonii* suggested 5 potentially co-regulated metabolites, with ILA as the sole metabolite that could be produced by *L. johnsonii* (Fig. 4D). Correlation's analysis of gut microbiota, metabolites, and colitis-related parameters provides evidence supporting the roles of *Lactobacillus* and ILA in mitigating colitis (Fig. 4E).

Previous studies have indicated that *Lactobacillus* could metabolize tryptophan into indole derivatives, most of which are known to be AhR agonists [46]. To better understand the specific metabolites responsible for activating the AhR pathway, targeted LC-MS/MS analysis was performed to determine the levels of tryptophan and related indole derivatives in different groups. Among these indole derivatives, ILA showed a significant increase in *L. johnsonii* intervention and had the highest content (Fig. 4F). Additionally, levels of ILA were increased in the BG + DSS group compared to DSS group (Fig. S6J). Although SCFAs, especially butyrate, have been shown to enhance AhR activation in cooperation with indole derivatives [47], we found that neither the levels of SCFAs nor gene expression of SCFA-associated receptors changed significantly in mice treated with

L. johnsonii or BG (Fig. S6K–N). Therefore, ILA, rather than other indole derivatives or SCFAs, plays a key role in activating AhR.

To establish the association between increased ILA levels and *L. johnsonii*, we conducted a comparative analysis of ILA production among different *Lactobacillus* species. Our findings demonstrated that *L. johnsonii* exhibited a superior capacity for ILA production compared to other *Lactobacillus* species (Fig. S6O). Furthermore, robust evidence from *L. johnsonii* colonization experiments in both GF and SPF mice confirmed the ability of *L. johnsonii* to increase ILA concentration in the intestinal tract (Fig. 4G–L).

Given the observed enrichment of ILA in *L. johnsonii*- and BG-treated mice, we proceeded to investigate the potential effects of ILA on colitis (Fig. 4M). Compared to the vehicle group, mice in the ILA group exhibited less body weight loss, lower DAI scores, and longer colon length (Fig. 4N–Q). Administration of ILA restored intestinal epithelial cell damage, rescued goblet cell numbers, and increased Muc2 protein expression (Fig. 4R, S). However, these beneficial effects of ILA were significantly attenuated when AhR was blocked (Fig. 4N–S). ILA treatment activated *Cyp1a1* and *Il22* expression, whereas the administration of CH223191 abolished this effect (Fig. 4T), thus indicating that AhR is necessary for this response. Additionally, ILA treatment reduced colonic levels of TNF-α and IL-6 while increasing IL-22 levels (Fig. 4U). These data demonstrate the protective effects of ILA on DSS-induced colitis through an AhR activation-dependent mechanism. Collectively, our findings highlight the role of the *L. johnsonii*–ILA–AhR axis in alleviating colitis by BG.

Growth of *L. johnsonii* depends on cross-feeding interaction with *B. uniformis* under BG supplementation

Although *Lactobacillus* has been identified as the primary beneficiary of BG degradation in both in vivo and in vitro studies [48, 49], our findings indicated that *L. johnsonii* cannot directly utilize BG, as it fails to grow in a basal media with BG as the sole carbon source (Fig. 5A, Fig. S7A). However, studies have suggested that the breakdown products of BG can promote the proliferation of *Lactobacillus* [50]. Co-occurrence network analysis confirmed positive correlations between *B. uniformis*, *Streptococcus*, *Enterococcus*, and *Turicibacter* with *Lactobacillus* (Fig. 5B). *Bacteroides* have a wide range of polysaccharide degradation capabilities [38], and upregulation of *B. uniformis* was observed in both BG-treated mice feces and in vitro fermented samples (Fig. 2D, I, Fig. S7B, C). There was a significant positive correlation between *B. uniformis* and *L. johnsonii* (Fig. 5C). Finally, we confirmed that *B. uniformis* is capable of degrading BG (Fig. 5D, Fig. S7D, E), and co-culturing *B. uniformis* with *L. johnsonii* in a basal medium with BG as the sole carbon source promoted the proliferation of *L. johnsonii* (Fig. 5E).

(See figure on next page.)

Fig. 5 The product of BG degradation by *B. uniformis* promotes the proliferation of *L. johnsonii*. **A**–**K** *B. uniformis* degraded BG and promoted the proliferation of *L. johnsonii*. For bacteria-related experiments, $n = 3$ per group; for animal-related experiments, $n = 6$ per group. **A** Growth curves of *L. johnsonii* in basal medium (without carbon source) containing BG or glucose as the sole carbon source. **B** Gut microbial co-occurrence network analysis based on core genus and species (average relative abundance > 0.1%) in the feces of mice (BG and vehicle groups). The red line indicates Spearman rank correlation coefficient > 0.30 and FDR-adjusted $P < 0.05$; the blue line indicates Spearman rank correlation coefficient < −0.30 and FDR-adjusted $P < 0.05$. **C** Spearman correlation between abundances of *B. uniformis* with *L. johnsonii* in feces of mice (BG + DSS and DSS groups). **D** Growth curves of *B. uniformis* in basal medium (BG or glucose as the sole carbon source). **E** The abundance of *L. johnsonii* after the co-culture of *B. uniformis* and *L. johnsonii* in the basal medium (BG as the sole carbon source) for 48 h. **F** Schematic of potential interaction between *B. uniformis* (BU) and *L. johnsonii* (LJ) via fermented products/metabolites. Briefly, BU was grown in basal medium (BG as the sole carbon source) for 48 h, followed by centrifugation of 4720 × g for 20 min at 4 °C. The supernatant was adjusted to pH 6.8 and sterilized by filtration (0.22 μm pore size) for inoculation of LJ. **G** Growth curves of *L. johnsonii* in basal medium (BG as the sole carbon source) with or without *B. uniformis* pre-culture for 24 h. **H** Metabolites profile in the supernatant at different time points. The purple lines indicate the metabolites that are increased during the growth of *B. uniformis* and decreased during the growth of *L. johnsonii*. **I** A heat map of the top 10 metabolites (based on the fold change value of LJ-24h/BU-48h) detected by untargeted metabolomics. **J** *T*-statistic of all detected metabolites by untargeted metabolomics. **K** Growth curve of *L. johnsonii* under the stimulation with different concentrations of NAM. **L** Experimental schema for **M**–**U**. Mice were treated with 100 mg/kg of NAM or PBS daily for 14 days, and 3% (w/v) DSS was added to the drinking water from day 7 to day 14. $n = 6$ mice per group. **M**, **N** Body weight (**M**) and disease activity index (**N**) were monitored daily after DSS treatment. **O** Representative photographs (left) and length quantification (right) of colon tissues. **P** Representative H&E-stained sections (upper) and AB/PAS-stained sections (lower) of the distal colon tissue. Scale bars, 100 μm. **Q** Histology score (left) was determined from H&E-stained sections, and the number of goblet cells per crypt (right) was determined from AB/PAS-stained sections. **R** The abundance of *L. johnsonii* in vehicle- and NAM-treated mice. **S** Relative gene expression of *Cyp1a1* and *Il22* in colon tissue assessed by RT-qPCR. **T** Colonic levels of IL-22. **U** Representative Muc2-stained colon sections (left) and quantified Muc2-positive area (right). Scale bars, 50 μm. Data are presented as the mean ± SEM. Statistical analysis was performed using *t*-test for **E** and **O**–**U** and two-way ANOVA followed by Bonferroni's post hoc test for **K**–**N**

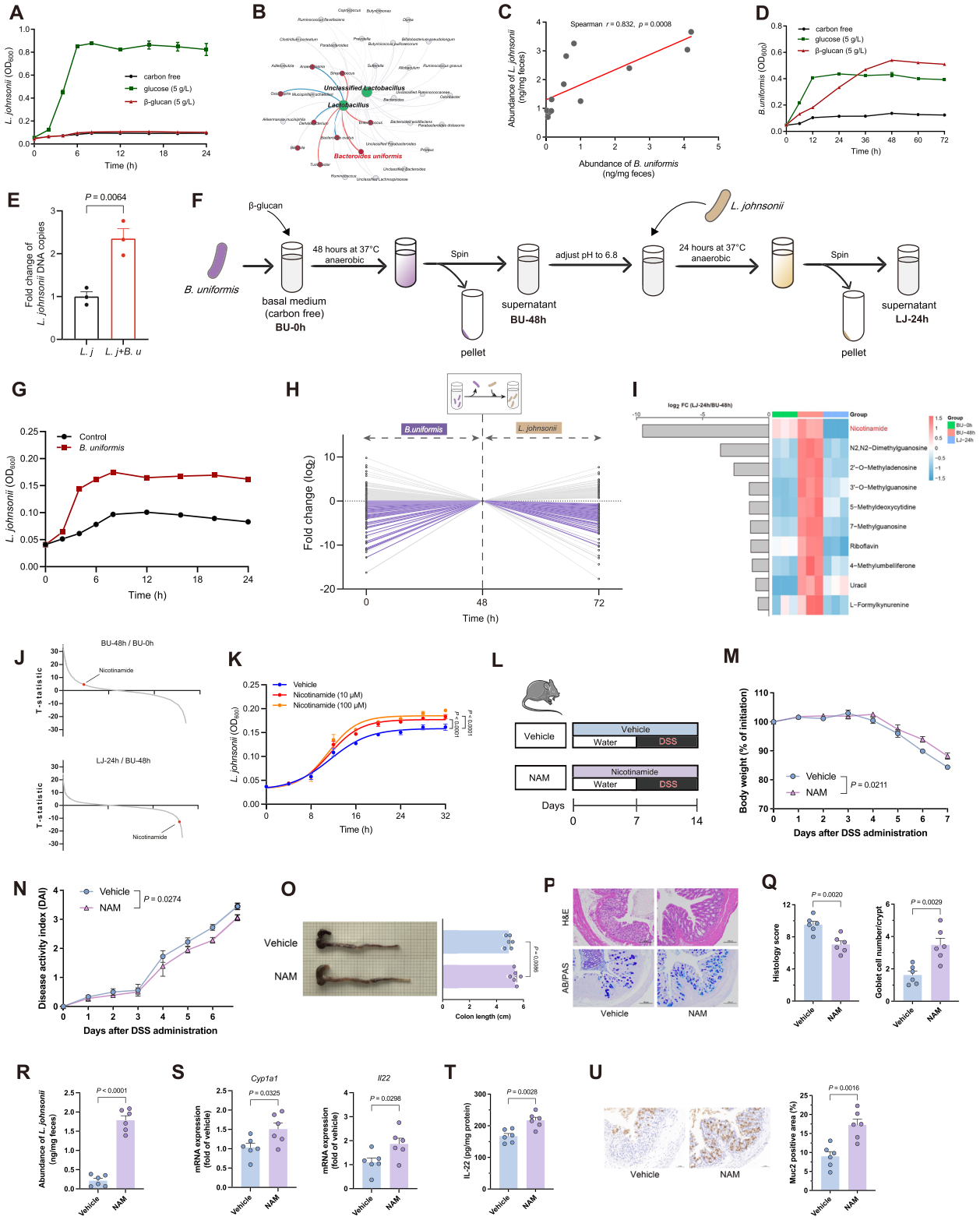

Fig. 5 (See legend on previous page.)

To provide direct evidence that *L. johnsonii* can benefit and proliferate from the degradation of BG by *B. uniformis*, we cultured *L. johnsonii* in the supernatant of *B. uniformis* growth medium for 48 h, with BG as the sole carbon source in the medium (Fig. 5F). We observed the proliferation of *L. johnsonii* along with the utilization of carbon sources, indicating that fermentation products of BG by *B. uniformis* serve as growth substrates for *L. johnsonii* proliferation (Fig. 5G, Fig. S7F, G). Since disaccharides, trisaccharides, and tetrasaccharides were minimally consumed, this suggested that glucose may be the primary BG fragment utilized by *L. johnsonii* (Fig. S7G).

During bacterial growth, a range of metabolic byproducts are produced, including organic acid, ammonia, sulfur compounds, phenols, and vitamins [51]. Since *L. johnsonii* can only utilize glucose generated from BG degradation by *B. uniformis*, we hypothesized that metabolic byproducts produced by *B. uniformis* are also potentially beneficial to the growth of *L. johnsonii*. Therefore, we characterized the metabolic profiles of basal medium, the supernatant of *B. uniformis* cultured for 48 h, and the supernatant of *L. johnsonii* cultured for 24 h (Fig. 5F). A profound distinction between the three groups was observed (Fig. S7H). Of all the metabolites, the ones produced by *B. uniformis* and utilized by *L. johnsonii* were particularly intriguing (Fig. 5H, purple lines). One compound of interest was NAM, which was almost completely depleted after culturing *L. johnsonii* (Fig. 5I, J, Fig. S7I). Furthermore, in vitro experiments demonstrated that NAM could be produced by *B. uniformis* and utilized by *L. johnsonii* (Fig. S7J–L). Adding NAM to diluted MRS significantly accelerated the growth of *L. johnsonii* (Fig. 5K). In contrast, N2,N2-dimethylguanosine and 2′-O-methyladenosine also showed significant reduction during *L. johnsonii* cultivation but had no impact on *L. johnsonii* growth (Fig. S7M, N). To establish the relationship between NAM and the promotion of *L. johnsonii* growth, we conducted NAM stimulation experiments on different *Lactobacillus* species and core intestinal bacteria. The results showed that NAM did not exhibit a significant growth-promoting effect on these bacteria (Fig. S7O).

To determine the in vivo effect of NAM in promoting *L. johnsonii* proliferation and alleviating colitis, we administered NAM to DSS-induced colitic mice. Our findings indicate that NAM could mitigate weight loss, reduce DAI, improve colon length, ameliorate histopathological changes, and preserve the number of goblet cells (Fig. 5L–Q). The efficacy of NAM, however, is dependent on certain bacterial strains, as it was ineffective when the gut microbiota in mice was depleted by antibiotics (Fig. S7P–U). We observed a significant increase in *L. johnsonii* in the fecal samples of NAM-treated mice (Fig. 5R). Additionally, the expression of *Cyp1a1* and *Il22*, as well as the colonic level of IL-22 and Muc2 proteins, was upregulated in the colon tissues of these mice (Fig. 5S–U). These results confirm that NAM promoted the proliferation of *L. johnsonii* in vivo and alleviates colitis, with a mechanism similar to that of *L. johnsonii*.

cobB gene mediates the production of NAM in *B. uniformis* and the growth of *L. johnsonii* in alleviating colitis

To test whether the growth promotion of *L. johnsonii* by *B. uniformis* depends on the production of NAM, we generated a NAM-synthesis-deficient strain of *B. uniformis* (BU△*cobB*) by knocking out the *cobB* gene

(See figure on next page.)

Fig. 6 Effect of BUΔ*cobB* on *L. johnsonii* and the effect of BG supplementation on target bacteria and metabolites in healthy individuals. **A** The biosynthesis genes of nicotinamide in the genome of *B. uniformis* (the results are based on protein BLAST searches by using the published genomes). **B** Verification of BUΔ*cobB*. **C** Growth curve of BU and BUΔ*cobB* on BHI medium. $n = 3$ for each group. **D** The intensity of NAM produced by BU and BUΔ*cobB* at the indicated time points. $n = 3$ for each group. **E** The abundance of *L. johnsonii* after the co-culture of BU or BUΔ*cobB* with *L. johnsonii* in the basal medium (BG as the sole carbon source) for 48 h. $n = 3$ for each group. **F** Experimental schema for **G**–**P**. Mice were treated with 1×10^8 CFU of vehicle, BU, or BUΔ*cobB* for 14 days, and 3% (w/v) DSS was added to the drinking water from day 7 to day 14. $n = 6$ mice per group. **G** Colonization of BU and BUΔ*cobB* strains in the feces of colitic mice. **H** The intensity of NAM in colonic content of different groups of mice. **I** The abundance of *L. johnsonii* in the feces of different groups of mice. **J**, **K** Body weight (J) and disease activity index (K) were monitored daily after DSS treatment. **L** Representative photographs (left) and length quantification (right) of colon tissues. **M** Representative H&E-stained sections (upper), AB/PAS-stained sections (middle), and immunocytochemistry of Muc2-stained sections (lower) of the distal colon tissue. Scale bars, 100 μm. **N** Histology score (left), the number of goblet cells per crypt (center), and quantified Muc2 positive area (right) of sections. **O** Relative gene expression of *Cyp1a1* and *Il22* in colon tissue assessed by RT-qPCR. **P** Colonic levels of MPO, TNF-α, IL-6, and IL-22. **Q**–**T** BG supplementation in healthy subjects. $n = 30$. **Q** The abundance of *L. johnsonii* (left) and *B. uniformis* (right) in feces at day 0 and day 14 of BG supplementation. **R** The level of ILA in feces at day 0 and day 14 of BG supplementation. **S** Spearman correlation between the abundance of *L. johnsonii* and the level of ILA at day 14 of BG supplementation. **T** Spearman correlation between the abundance of *L. johnsonii* and *B. uniformis* at day 14 of BG supplementation. Data are presented as the mean ± SEM. Statistical analysis was performed using *t*-test for **D**, one-way ANOVA followed by Tukey's post hoc test for **E** and **L**, **M**–**P**; Kruskal–Wallis test for **G**–**I**; two-way ANOVA followed by Tukey's post hoc test for **J** and **K**; and Mann–Whitney test for **Q**–**T**

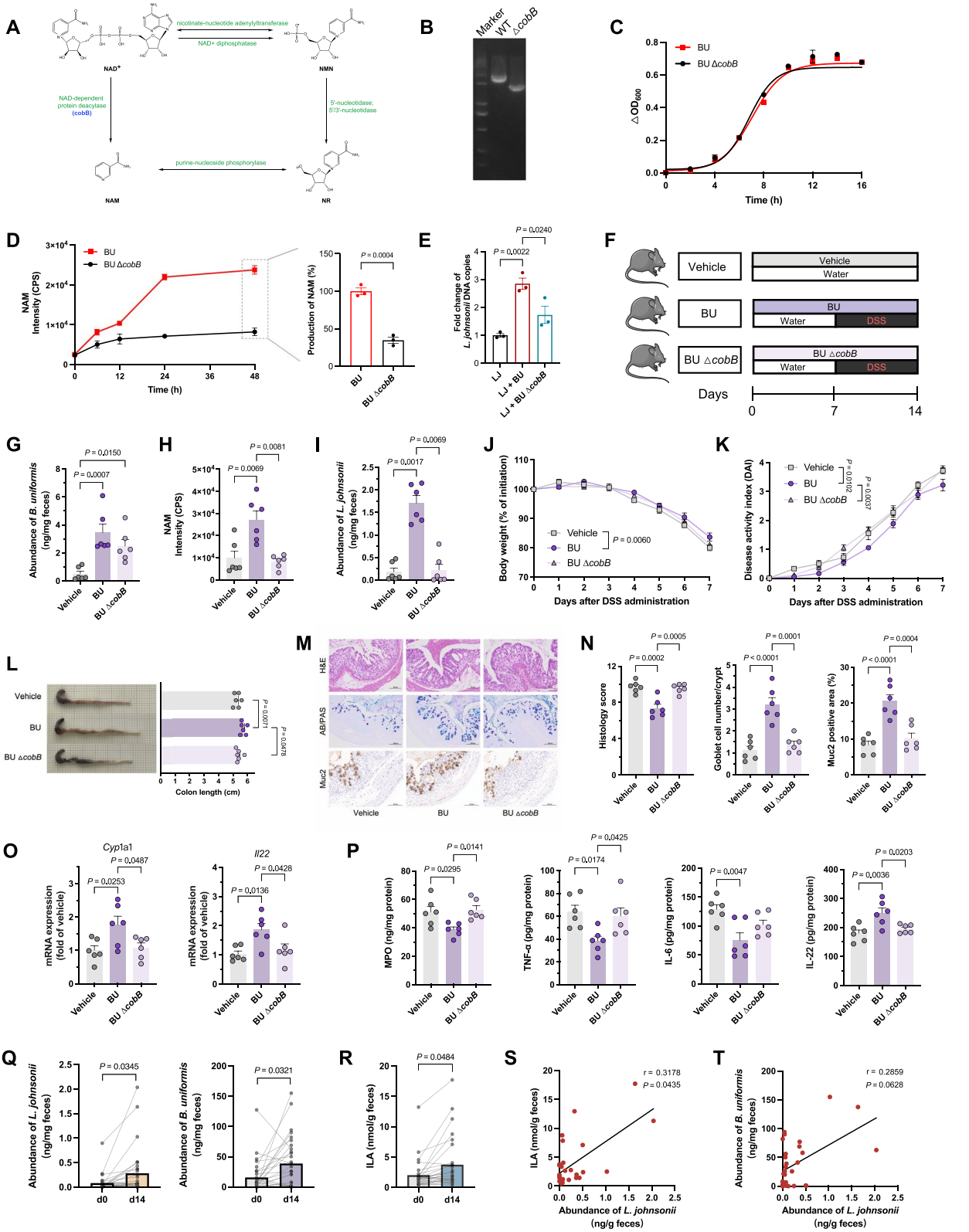

Fig. 6 (See legend on previous page.)

involved in regulating nicotinamide adenine dinucleotide (NAD+) metabolism, which directly affects NAM biosynthesis (Fig. 6A–C). The LC-MS/MS results confirmed a significant decrease in NAM production in BU△*cobB* (Fig. 6D). In vitro co-culturing of BU△*cobB* with *L. johnsonii* showed a significant decrease in the ability to promote *L. johnsonii* proliferation when compared to the wild-type *B. uniformis* (BU) (Fig. 6E). The administration of BU and BU△*cobB* to mice confirmed that NAM production was essential for *B. uniformis* to promote *L. johnsonii* growth in vivo (Fig. 6F–I). The results also suggest that NAM production in *B. uniformis* plays a crucial role in alleviating colitis symptoms, upregulating the expression of *Cyp1a1* and *Il22*, decreasing the level of MPO, TNF-α, and IL-6, as well as increasing the level of IL-22 (Fig. 6J–P). In contrast, BU△*cobB* could not activate the AhR pathway or alleviate inflammation (Fig. 6J–P). These findings demonstrate the critical role of NAM produced by *B. uniformis* in promoting *L. johnsonii* growth.

Proof-of-concept clinical validation

The deficiency of AhR ligands in patients with IBD is considered to contribute to the development of the disease, and dietary interventions highlight treatment before disease onset [10, 52]. To investigate whether the interaction between *B. uniformis* and *L. johnsonii* in response to BG supplementation could causally influence ILA production, we conducted a 2-week single-arm interventional study in healthy adults. As expected, supplementation with BG led to a significant increase in the abundance of *L. johnsonii* and *B. uniformis* in fecal samples (Fig. 6Q). Importantly, it was accompanied by a concurrent and significant elevation in fecal ILA levels (Fig. 6R). Correlation analysis further revealed a significant positive association between the abundance of *L. johnsonii* and ILA levels (Fig. 6S), supporting our previous observations in murine models. Additionally, a positive trend was observed between the abundance of *B. uniformis* and *L. johnsonii*, though this relationship did not reach statistical significance, possibly due to the high degree of individual intestinal microbiota heterogeneity (Fig. 6T). Collectively, these findings indicate that BG supplementation holds promise as a strategy to increase *L. johnsonii* abundance and ILA levels in the gut.

Discussion

Research has established a link between Western diet and the onset of IBD [53], while a high-fiber diet can reduce the risk of IBD or improve the quality of life in IBD patients by reshaping the gut microbiota [54, 55]. BG, a common dietary fiber, has been shown to ameliorate colitis [56, 57], but the underlying mechanisms remain unclear. Here, we demonstrate that *L. johnsonii* is a key bacterium mediating the beneficial effects of BG on colitis, as it can produce substantial amounts of ILA that activate the AhR signaling pathway. Furthermore, *B. uniformis* can degrade BG and produce NAM, which is critical for promoting the proliferation of *L. johnsonii*.

Although recent studies have provided increasing evidence that BG can significantly influence the gut microbiome and its metabolites [58, 59], the key bacteria and metabolites mediating the anti-inflammatory effects of BG in the gut remain unknown. Through a series of in vivo and in vitro experiments, we confirmed the targeted enrichment effect of BG on *Lactobacillus*, especially *L. johnsonii*. Similarly, BG derived from *Schizophyllum commune* has been shown to ameliorate obesity-associated colitis and increase the abundance of *Lactobacillus* [60]. Numerous studies have also reported that BG can induce an increase of *Lactobacillus* abundance in metabolic syndrome mice [61], normal rats [62], and in vitro fermentation using fecal samples from normal mice or humans [59, 63]. However, these reports have rarely provided information at the species level. Here, we found that *L. johnsonii* is the major *Lactobacillus* species enriched by BG, and its abundance is also significantly increased in recipient mice after FMT, suggesting its important role in BG alleviation of colitis.

Lactobacillus generally possesses the ability to degrade tryptophan into indole derivatives. Several of these indole derivatives, including ILA, indole-3-acrylic acid, indole-3-acetic acid, and indole-3-aldehyde, have been shown to act as agonists of the AhR [46]. Specifically, ILA can activate the AhR in human $CD4^+$ T cells isolated under Th17 polarizing conditions, promoting the production of the anti-inflammatory cytokine IL-22 [64]. This study revealed that *L. johnsonii* has a strong ILA-producing capacity and is superior to other *Lactobacillus* spp. Importantly, our results also indicate a marked upregulation of ILA levels in the gut of mice after BG intervention. This suggests that *L. johnsonii*, as the predominant bacterium enriched by BG, plays a significant role in shaping the gut metabolite profile. These findings are consistent with a previous study showing that BG treatment ameliorated colitis in mice and induced an enrichment of the tryptophan metabolism pathway in the gut, which was positively correlated with the increased *Lactobacillus* abundance [65].

Bacterial degradation of dietary fiber can also result in the production of SCFAs and have beneficial effects on host health [66]. However, this study found no significant changes in the SCFA levels or SCFA-sensing receptor

activation after BG intervention in mice. Similar findings have been previously reported in both murine and human studies [67–69]. This phenomenon may be attributable to the cross-feeding interactions between gut microbiota that facilitate rapid SCFA consumption and dynamic homeostatic regulation [70]. Furthermore, the intestinal environment and structure of gut microbiota may also influence SCFA production [70]. Therefore, the role of BG in mitigating colitis is probable not due to SCFA but primarily to ILA.

We next elucidated the key reasons for the proliferation of *L. johnsonii*. This study found that *L. johnsonii* cannot directly utilize BG for growth, consistent with previous research [71]. Interestingly, within the complex gut environment, bacteria can cross-feed using their metabolic byproducts [72]. However, the intricacies of bacterial metabolic patterns remain a challenge in this area of research. Here, we reveal a cross-feeding between *B. uniformis* and *L. johnsonii*, whereby the glucose and NAM produced by *B. uniformis* during the degradation of BG served as energy sources for *L. johnsonii*. It has been reported that *B. uniformis* possesses polysaccharide utilization loci (PULs), such as the BACOVA_02741-02745, which enable the breakdown of BG into glucose [38]. Importantly, NAM is an important precursor of NAD+, which participates in multiple energy metabolism pathways and is critical for bacterial proliferation [73]. Studies have shown that lactobacilli can convert NAM into NAD+by nicotinamidase and nicotinate phosphoribosyltransferase [74, 75]. This suggests that *L. johnsonii* may utilize NAM by a similar mechanism to promote its proliferation, but the exact mechanism needs to be further investigated.

Clinical research reports indicate that IBD patients exhibit lower levels of AhR ligands in the gut compared to healthy controls [10, 76]. *Lactobacillus* contributes to the level of AhR ligands in the gut. However, IBD patients generally exhibit a reduced abundance of *Lactobacillus* [77], and the fecal ILA levels are negatively correlated with the severity of disease [78]. It is reported that a mixture containing BG has beneficial effects on IBD patients [56]. Moreover, our study found that BG supplementation increased the abundance of *L. johnsonii* and fecal ILA levels in healthy individuals. Previous clinical trials have also reported that oats and oat flour containing BG can boost *Lactobacillus* levels in the feces of healthy individuals with mildly elevated cholesterol [48, 49]. Additionally, regarding our finding of cross-feeding between *B. uniformis* and *L. johnsonii*, it has also been reported that BG supplementation can increase *Bacteroides* abundance in individuals [79]. Therefore, increasing *Lactobacillus* abundance and AhR ligand levels through BG administration may be a promising strategy for IBD management.

The limitations of this study need to be discussed. Although we observed the ameliorating effect of BG on colitis in mice and explored the underlying mechanisms, the critical role of ILA production in *L. johnsonii* could be better confirmed through the use of ILA-deficient strains. In addition, the detailed mechanism by which NAM promotes the growth of *L. johnsonii*, as well as the clinical application of BG in IBD patients, warrants deeper investigation and verification in the future.

Conclusion

Our study elucidated the mechanism underlying the beneficial effects of BG in colitis and provided insights into bacterial cross-feeding. Specifically, *B. uniformis* was found to degrade BG, leading to the production of NAM, which in turn promoted the proliferation of *L. johnsonii*. The amelioration of colitis by BG was shown to depend on the activation of the AhR signaling pathway, mediated by ILA primarily derived from *L. johnsonii*. This study highlights the significance of bacterial metabolism and cross-feeding in modulating host health by bioactive dietary compounds. The identified key bacterial strains and metabolites offer valuable insights for the development of strategies for managing IBD, and the utilization of BG as a functional food ingredient holds potential for the creation of innovative dietary interventions to promote intestinal health.

Abbreviations

AB/PAS	Alcian Blue/periodic acid-Schiff
ATCC	American Type Culture Collection
AhR	Aryl hydrocarbon receptor
BG	*β*-Glucan
BHI	Brain heart infusion
DAI	Disease activity index
DEGs	Differentially expressed genes
DSS	Dextran sulfate sodium
ELISA	Enzyme-linked immunosorbent assay
FDR	False discovery rate
FMT	Fecal microbiota transplantation
GF	Germ-free
H&E	Hematoxylin and eosin
IBD	Inflammatory bowel disease
ILA	Indole-3-lactic acid
LDA	Linear discriminant analysis
LEfSe	Linear discriminant analysis effect size
LJCS	*L. johnsonii* Cultured supernatant
MPO	Myeloperoxidase
MRM	Multiple reaction monitoring
MRS	Man-Rogosa-Sharpe
NAD+	Nicotinamide adenine dinucleotide
NAM	Nicotinamide
SCFAs	Short-chain fatty acids
SEM	Standard error of the mean
SPF	Specific pathogen-free

Supplementary Information

The online version contains supplementary material available at https://doi.org/10.1186/s40168-024-01896-9.

Supplementary Material 1: Supplementary figures: Figure S1. The effect of BG on gut microbiota. Figure S2. Microbiota depletion with antibiotics eliminated the alleviating effect of BG on colitis. Figure S3. Fecal microbial transplantation of BG-regulated microbiota mitigates DSS-induced colitis. Figure S4. BG has an enrichment effect on *L. johnsonii*. Figure S5. Inhibition of the AhR signaling pathway abolishes the effect of *L. johnsonii* and BG on colitis. Figure S6. Analysis of the non-target metabolome of culture supernatant and colonic contents of *L. johnsonii*-treated mice. Figure S7. *B. uniformis* promotes the proliferation of *L. johnsonii* (in vivo and in vitro). Supplementary tables: Table S1. Primer sequences for real-time PCR of target genes used in the study. Table S2. Primer sequences for real-time qPCR analysis of target bacteria

Acknowledgements
We thank Dr. Kai Wang (Peking University) and Dr. Yong Ding (Peking University) for their valuable suggestions and technical support for the manuscript.

Authors' contributions
S.Z., Q.N., Y.S., and S.N. conceived and designed the study. S.Z., Q.N., Y.S., S.Z., C.C., S.L., J.Y., J.H., X.Z., Y.Y., P.H., and L.L. performed the experiments. S.Z., Q.N., Y.S. wrote the manuscript, prepared the figures, and was responsible for data compilation and integration. M.X. and S.N. guided the project, provided funding support, and revised the manuscript. All authors reviewed the manuscript.

Funding
This work was supported by the National Natural Science Foundation of China for the Key Project of International Cooperative Research (32120103012), the National Natural Science Foundation of China for Distinguished Young Scholars (31825020), the Young Elite Scientists Sponsorship Program by JXAST (2023QT01), the Technological Project of Jiangxi Province (20232BCD44003), the Technological Innovation Guidance Science and Technology Project of Jiangxi Province (20203AEI007), the Key Technological Project of Jiangxi Province (20212AAF01005), the Key Laboratory of Bioactive Polysaccharides of Jiangxi Province (20212BCD42016), and the Postdoctoral Fellowship Program (Grade B) of China Postdoctoral Science Foundation (GZB20230285).

Availability of data and materials
The 16S rRNA gene sequencing raw sequence reads (fastq) and RNA-seq sequencing data produced in this study are available in the NCBI Sequence Read Archive under accession projects PRJNA1040335 and PRJNA1073251, respectively. Non-targeted metabolomic data are available in the Metabolights database under accession projects MTBLS8950. All other data is contained within the main manuscript and supplemental files.

Declarations

Ethics approval and consent to participate
All animal experiments were performed under the Guidelines for Care and Use of Laboratory Animals of the National Institutes of Health and were approved by the Experimental Animal Care and Use Committee of Nanchang University, number IACUC-20221030001. The study involving human participants was approved by the Ethics Committee of the First Affiliated Hospital of Nanchang University, number IIT2022077. The trial was registered at the Chinese Clinical Trial Registry, number ChiCTR2200066468.

Consent for publication
Not applicable.

Competing interests
The authors declare no competing interests.

Author details
[1]State Key Laboratory of Food Science and Resources, China-Canada Joint Lab of Food Science and Technology, Key Laboratory of Bioactive Polysaccharides of Jiangxi Province, Nanchang University, Nanchang, China. [2]Department of Nutrition, the First Affiliated Hospital of Nanchang University, Nanchang, China.

Received: 15 January 2024 Accepted: 30 July 2024
Published online: 19 September 2024

References

1. Ananthakrishnan AN, Bernstein CN, Iliopoulos D, Macpherson A, Neurath MF, Ali RAR, Vavricka SR, Fiocchi C. Environmental triggers in IBD: a review of progress and evidence. Nat Rev Gastroenterol Hepatol. 2018;15(1):39–49.
2. Zmora N, Suez J, Elinav E. You are what you eat: diet, health and the gut microbiota. Nat Rev Gastroenterol Hepatol. 2019;16(1):35–56.
3. Ananthakrishnan AN, Khalili H, Konijeti GG, Higuchi LM, De Silva P, Korzenik JR, Fuchs CS, Willett WC, Richter JM, Chan AT. A prospective study of long-term intake of dietary fiber and risk of Crohn's disease and ulcerative colitis. Gastroenterology. 2013;145(5):970–7.
4. Ott SJ, Musfeldt M, Wenderoth DF, Hampe J, Brant O, Folsch UR, Timmis KN, Schreiber S. Reduction in diversity of the colonic mucosa associated bacterial microflora in patients with active inflammatory bowel disease. Gut. 2004;53(5):685–93.
5. Machiels K, Joossens M, Sabino J, De Preter V, Arijs I, Eeckhaut V, Ballet V, Claes K, Van Immerseel F, Verbeke K, et al. A decrease of the butyrate-producing species Roseburia hominis and Faecalibacterium prausnitzii defines dysbiosis in patients with ulcerative colitis. Gut. 2014;63(8):1275–83.
6. Schirmer M, Garner A, Vlamakis H, Xavier RJ. Microbial genes and pathways in inflammatory bowel disease. Nat Rev Microbiol. 2019;17(8):497–511.
7. Lloyd-Price J, Arze C, Ananthakrishnan AN, Schirmer M, Avila-Pacheco J, Poon TW, Andrews E, Ajami NJ, Bonham KS, Brislawn CJ. Multi-omics of the gut microbial ecosystem in inflammatory bowel diseases. Nature. 2019;569(7758):655–62.
8. Krautkramer KA, Fan J, Bäckhed F. Gut microbial metabolites as multi-kingdom intermediates. Nat Rev Microbiol. 2021;19(2):77–94.
9. Lavelle A, Sokol H. Gut microbiota-derived metabolites as key actors in inflammatory bowel disease. Nat Rev Gastroenterol Hepatol. 2020;17(4):223–37.
10. Lamas B, Richard ML, Leducq V, Pham H-P, Michel M-L, Da Costa G, Bridonneau C, Jegou S, Hoffmann TW, Natividad JM. CARD9 impacts colitis by altering gut microbiota metabolism of tryptophan into aryl hydrocarbon receptor ligands. Nat Med. 2016;22(6):598–605.
11. Busbee PB, Menzel L, Alrafas HR, Dopkins N, Becker W, Miranda K, Tang C, Chatterjee S, Singh UP, Nagarkatti M. Indole-3-carbinol prevents colitis and associated microbial dysbiosis in an IL-22–dependent manner. JCI insight. 2020;5(1):e127551.
12. Ratiner K, Ciocan D, Abdeen SK, Elinav E. Utilization of the microbiome in personalized medicine. Nat Rev Microbiol. 2024;22(5):291–308.
13. Christensen C, Knudsen A, Arnesen EK, Hatlebakk JG, Sletten IS, Fadnes LT. Diet, food, and nutritional exposures and inflammatory bowel disease or progression of disease: an umbrella review. Adv Nutr. 2024;15(5):100219.
14. Food, Drug Administration, H. Food labeling: health claims; soluble fiber from certain foods and risk of coronary heart disease Final rule. Fed Regist. 2008;73(85):23947–53.
15. Liu B, Lin Q, Yang T, Zeng L, Shi L, Chen Y, Luo F. Oat β-glucan ameliorates dextran sulfate sodium (DSS)-induced ulcerative colitis in mice. Food Funct. 2015;6(11):3454–63.
16. Wang Y-X, Li L-Y, Zhang T, Wang J-Q, Huang X-J, Hu J-L, Yin J-Y, Nie S-P. Fractionation, physicochemical and structural characterization of polysaccharides from barley water-soluble fiber. Food Hydrocolloids. 2021;113:106539.
17. Nie Q, Hu J, Gao H, Li M, Sun Y, Chen H, Zuo S, Fang Q, Huang X, Yin J. Bioactive dietary fibers selectively promote gut microbiota to exert antidiabetic effects. J Agric Food Chem. 2021;69(25):7000–15.
18. Sugimura N, Li Q, Chu ESH, Lau HCH, Fong W, Liu W, Liang C, Nakatsu G, Su ACY, Coker OO, et al. Lactobacillus gallinarum modulates the gut microbiota and produces anti-cancer metabolites to protect against colorectal tumourigenesis. Gut. 2021;71(1):2011–21.

19. Negi G, Kumar A, Kaundal RK, Gulati A, Sharma SS. Functional and biochemical evidence indicating beneficial effect of Melatonin and Nicotinamide alone and in combination in experimental diabetic neuropathy. Neuropharmacology. 2010;58(3):585–92.
20. Wirtz S, Popp V, Kindermann M, Gerlach K, Weigmann B, Fichtner-Feigl S, Neurath MF. Chemically induced mouse models of acute and chronic intestinal inflammation. Nat Protoc. 2017;12(7):1295–309.
21. Sun Y, Nie Q, Zhang S, He H, Zuo S, Chen C, Yang J, Chen H, Hu J, Li S. Parabacteroides distasonis ameliorates insulin resistance via activation of intestinal GPR109a. Nat Commun. 2023;14(1):7740.
22. Bolyen E, Rideout JR, Dillon MR, Bokulich NA, Abnet CC, Al-Ghalith GA, Alexander H, Alm EJ, Arumugam M, Asnicar F. Reproducible, interactive, scalable and extensible microbiome data science using QIIME 2. Nat Biotechnol. 2019;37(8):852–7.
23. Callahan BJ, McMurdie PJ, Rosen MJ, Han AW, Johnson AJA, Holmes SP. DADA2: high-resolution sample inference from Illumina amplicon data. Nat Methods. 2016;13(7):581–3.
24. McDonald D, Price MN, Goodrich J, Nawrocki EP, DeSantis TZ, Probst A, Andersen GL, Knight R, Hugenholtz P. An improved Greengenes taxonomy with explicit ranks for ecological and evolutionary analyses of bacteria and archaea. ISME J. 2012;6(3):610–8.
25 Lu Y, Zhou G, Ewald J, Pang Z, Shiri T, Xia J. MicrobiomeAnalyst 2.0: comprehensive statistical, functional and integrative analysis of microbiome data. Nucleic Acids Res. 2023;51(W1):W310–8.
26. Segata N, Izard J, Waldron L, Gevers D, Miropolsky L, Garrett WS, Huttenhower C. Metagenomic biomarker discovery and explanation. Genome Biol. 2011;12:1–18.
27. Cáceres MD, Legendre P. Associations between species and groups of sites: indices and statistical inference. Ecology. 2009;90(12):3566–74.
28. Kim D, Paggi JM, Park C, Bennett C, Salzberg SL. Graph-based genome alignment and genotyping with HISAT2 and HISAT-genotype. Nat Biotechnol. 2019;37(8):907–15.
29. Love MI, Huber W, Anders S. Moderated estimation of fold change and dispersion for RNA-seq data with DESeq2. Genome Biol. 2014;15:1–21.
30. Dong F, Hao F, Murray IA, Smith PB, Koo I, Tindall AM, Kris-Etherton PM, Gowda K, Amin SG, Patterson AD. Intestinal microbiota-derived tryptophan metabolites are predictive of Ah receptor activity. Gut Microbes. 2020;12(1):1788899.
31 Nie Q, Sun Y, Hu W, Chen C, Lin Q, Nie S. Glucomannan promotes Bacteroides ovatus to improve intestinal barrier function and ameliorate insulin resistance. iMeta. 2024;3(1):e163.
32. Nie Q, Luo X, Wang K, Ding Y, Jia S, Zhao Q, Li M, Zhang J, Zhuo Y, Lin J. Gut symbionts alleviate MASH through a secondary bile acid biosynthetic pathway. Cell. 2024;187:1–18.
33. Poeker SA, Lacroix C, De Wouters T, Spalinger MR, Scharl M, Geirnaert A. Stepwise development of an in vitro continuous fermentation model for the murine caecal microbiota. Front Microbiol. 2019;10:1166.
34. Centanni M, Hutchison JC, Carnachan SM, Daines AM, Kelly WJ, Tannock GW, Sims IM. Differential growth of bowel commensal Bacteroides species on plant xylans of differing structural complexity. Carbohydr Polym. 2017;157:1374–82.
35. Dubois M, Gilles KA, Hamilton JK, Rebers PT, Smith F. Colorimetric method for determination of sugars and related substances. Anal Chem. 1956;28(3):350–6.
36. Zhang H, Zou P, Zhao H, Qiu J, Mac Regenstein J, Yang X. Isolation, purification, structure and antioxidant activity of polysaccharide from pinecones of Pinus koraiensis. Carbohydr Polym. 2021;251:117078.
37. Rivière A, Gagnon M, Weckx S, Roy D, De Vuyst L. Mutual cross-feeding interactions between Bifidobacterium longum subsp. longum NCC2705 and Eubacterium rectale ATCC 33656 explain the bifidogenic and butyrogenic effects of arabinoxylan oligosaccharides. Appl Environ Microbiol. 2015;81(22):7767–81.
38. Tamura K, Hemsworth GR, Déjean G, Rogers TE, Pudlo NA, Urs K, Jain N, Davies GJ, Martens EC, Brumer H. Molecular mechanism by which prominent human gut Bacteroidetes utilize mixed-linkage beta-glucans, major health-promoting cereal polysaccharides. Cell Rep. 2017;21(2):417–30.
39. Zelante T, Iannitti RG, Cunha C, De Luca A, Giovannini G, Pieraccini G, Zecchi R, D'Angelo C, Massi-Benedetti C, Fallarino F, et al. Tryptophan catabolites from microbiota engage aryl hydrocarbon receptor and balance mucosal reactivity via interleukin-22. Immunity. 2013;39(2):372–85.
40. Katakura K, Lee J, Rachmilewitz D, Li G, Eckmann L, Raz E. Toll-like receptor 9–induced type I IFN protects mice from experimental colitis. J Clin Investig. 2005;115(3):695–702.
41. Rees V. Chronic experimental colitis induced by dextran sulphate sodium (DSS) is characterized by Th1 and Th2 cytokines. Clin Exp Immunol. 1998;114(3):385–91.
42. Zhang C, Yu L, Ma C, Jiang S, Zhang Y, Wang S, Tian F, Xue Y, Zhao J, Zhang H. A key genetic factor governing arabinan utilization in the gut microbiome alleviates constipation. Cell Host Microbe. 2023;31(12):1989-2006.e8.
43. Chang C-S, Liao Y-C, Huang C-T, Lin C-M, Cheung CHY, Ruan J-W, Yu W-H, Tsai Y-T, Lin I-J, Huang C-H. Identification of a gut microbiota member that ameliorates DSS-induced colitis in intestinal barrier enhanced Dusp6-deficient mice. Cell Rep. 2021;37(8):110016.
44. Natividad JM, Agus A, Planchais J, Lamas B, Jarry AC, Martin R, Michel M-L, Chong-Nguyen C, Roussel R, Straube M. Impaired aryl hydrocarbon receptor ligand production by the gut microbiota is a key factor in metabolic syndrome. Cell Metab. 2018;28(5):737-49.e4.
45. Cervantes-Barragan L, Chai JN, Tianero MD, Di Luccia B, Ahern PP, Merriman J, Cortez VS, Caparon MG, Donia MS, Gilfillan S. Lactobacillus reuteri induces gut intraepithelial CD4+ CD8αα+ T cells. Science. 2017;357(6353):806–10.
46. Agus A, Planchais J, Sokol H. Gut microbiota regulation of tryptophan metabolism in health and disease. Cell Host Microbe. 2018;23(6):716–24.
47. Yang W, Yu T, Huang X, Bilotta AJ, Xu L, Lu Y, Sun J, Pan F, Zhou J, Zhang W. Intestinal microbiota-derived short-chain fatty acids regulation of immune cell IL-22 production and gut immunity. Nat Commun. 2020;11(1):1–18.
48. Duysburgh C, Van den Abbeele P, Kamil A, Fleige L, De Chavez PJ, Chu Y, Barton W, O'Sullivan O, Cotter PD, Quilter K, et al. In vitro-in vivo validation of stimulatory effect of oat ingredients on Lactobacilli. Pathogens. 2021;10(2):235.
49. Kamil A, Fleige L, Chu Y, Chavez PJD, Duysburgh C, Van den Abbeele P. Oats containing 1.4 g β-glucan significantly increased Lactobacillus levels in vitro using M-SHIME® model and in vivo in healthy adults with elevated cholesterol levels. Curr Dev Nutr. 2020;4(Supplement_2):nzaa062_24.
50. Golisch B, Lei Z, Tamura K, Brumer H. Configured for the human gut microbiota: molecular mechanisms of dietary β-glucan utilization. ACS Chem Biol. 2021;16(11):2087–102.
51. Oliphant K, Allen-Vercoe E. Macronutrient metabolism by the human gut microbiome: major fermentation by-products and their impact on host health. Microbiome. 2019;7(1):91.
52. Van de Guchte M, Blottière HM, Doré J. Humans as holobionts: implications for prevention and therapy. Microbiome. 2018;6(1):1–6.
53. Hou JK, Abraham B, El-Serag H. Dietary intake and risk of developing inflammatory bowel disease: a systematic review of the literature. ACG. 2011;106(4):563–73.
54. Fritsch J, Garces L, Quintero MA, Pignac-Kobinger J, Santander AM, Fernández I, Ban YJ, Kwon D, Phillips MC, Knight K. Low-fat, high-fiber diet reduces markers of inflammation and dysbiosis and improves quality of life in patients with ulcerative colitis. CGH. 2021;19(6):1189–99.
55. Milajerdi A, Ebrahimi-Daryani N, Dieleman LA, Larijani B, Esmaillzadeh A. Association of dietary fiber, fruit, and vegetable consumption with risk of inflammatory bowel disease: a systematic review and meta-analysis. Adv Nutr. 2021;12(3):735–43.
56. Spagnuolo R, Cosco C, Mancina RM, Ruggiero G, Garieri P, Cosco V, Doldo P. Beta-glucan, inositol and digestive enzymes improve quality of life of patients with inflammatory bowel disease and irritable bowel syndrome. Eur Rev Med Pharmacol Sci. 2017;21(2 Suppl):102–7.
57. Hallert C, Björck I, Nyman M, Pousette A, Grännö C, Svensson H. Increasing fecal butyrate in ulcerative colitis patients by diet: controlled pilot study. Inflamm Bowel Dis. 2003;9(2):116–21.
58. Fernandez-Julia PJ, Munoz-Munoz J, van Sinderen D. A comprehensive review on the impact of β-glucan metabolism by Bacteroides and Bifidobacterium species as members of the gut microbiota. Int J Biol Macromol. 2021;181:877–89.
59. Bai J, Li T, Zhang W, Fan M, Qian H, Li Y, Wang L. Systematic assessment of oat beta-glucan catabolism during in vitro digestion and fermentation. Food Chem. 2021;348:129116.
60. Vu V, Muthuramalingam K, Singh V, Hyun C, Kim YM, Unno T, Cho M. Effects of β-glucan, probiotics, and synbiotics on obesity-associated

colitis and hepatic manifestations in C57BL/6J mice. Eur J Nutr. 2022;61:793–807.
61. Chen G, Chen D, Zhou W, Peng Y, Chen C, Shen W, Zeng X, Yuan Q. Improvement of metabolic syndrome in high-fat diet-induced mice by yeast β-glucan is linked to inhibited proliferation of Lactobacillus and Lactococcus in gut microbiota. J Agric Food Chem. 2021;69(27):7581–92.
62. Snart J, Bibiloni R, Grayson T, Lay C, Zhang H, Allison GE, Laverdiere JK, Temelli F, Vasanthan T, Bell R. Supplementation of the diet with high-viscosity beta-glucan results in enrichment for lactobacilli in the rat cecum. Appl Environ Microbiol. 2006;72(3):1925–31.
63. Dong JL, Yang M, Zhu YY, Shen RL, Zhang KY. Comparative study of thermal processing on the physicochemical properties and prebiotic effects of the oat beta-glucan by in vitro human fecal microbiota fermentation. Food Res Int. 2020;138(Pt B):109818.
64. Laursen MF, Sakanaka M, von Burg N, Mörbe U, Andersen D, Moll JM, Pekmez CT, Rivollier A, Michaelsen KF, Mølgaard C. Bifidobacterium species associated with breastfeeding produce aromatic lactic acids in the infant gut. Nat Microbiol. 2021;6(11):1367–82.
65. Liu C, Sun C, Cheng Y. β-glucan alleviates mice with ulcerative colitis through interactions between gut microbes and amino acids metabolism. J Sci Food Agric. 2023;103(8):4006–16.
66. Xu T, Wu X, Liu J, Sun J, Wang X, Fan G, Meng X, Zhang J, Zhang Y. The regulatory roles of dietary fibers on host health via gut microbiota-derived short chain fatty acids. Curr Opin Pharmacol. 2022;62:36–42.
67. Wu T-R, Lin C-S, Chang C-J, Lin T-L, Martel J, Ko Y-F, Ojcius DM, Lu C-C, Young JD, Lai H-C. Gut commensal Parabacteroides goldsteinii plays a predominant role in the anti-obesity effects of polysaccharides isolated from Hirsutella sinensis. Gut. 2019;68(2):248–62.
68. Li H, Zhang L, Li J, Wu Q, Qian L, He J, Ni Y, Kovatcheva-Datchary P, Yuan R, Liu S. Resistant starch intake facilitates weight loss in humans by reshaping the gut microbiota. Nat Metab. 2024;6:578–97.
69 Vinelli V, Biscotti P, Martini D, Del Bo' C, Marino M, Meroño T, Nikoloudaki O, Calabrese FM, Turroni S, Taverniti V. Effects of dietary fibers on short-chain fatty acids and gut microbiota composition in healthy adults: a systematic review. Nutrients. 2022;14(13):2559.
70. Mann ER, Lam YK, Uhlig HH. Short-chain fatty acids: linking diet, the microbiome and immunity. Nat Rev Immunol. 2024;24:577–95.
71. Crittenden R, Karppinen S, Ojanen S, Tenkanen M, Fagerström R, Mättö J, Saarela M, Mattila-Sandholm T, Poutanen K. In vitro fermentation of cereal dietary fibre carbohydrates by probiotic and intestinal bacteria. J Sci Food Agric. 2002;82(8):781–9.
72. D'Souza G, Shitut S, Preussger D, Yousif G, Waschina S, Kost C. Ecology and evolution of metabolic cross-feeding interactions in bacteria. Nat Prod Rep. 2018;35(5):455–88.
73. Covarrubias AJ, Perrone R, Grozio A, Verdin E. NAD+ metabolism and its roles in cellular processes during ageing. Nat Rev Mol Cell Biol. 2021;22(2):119–41.
74. Lv X, Liu G, Sun X, Chen H, Sun J, Feng Z. Nutrient consumption patterns of Lactobacillus acidophilus KLDS 1.0738 in controlled pH batch fermentations. J Dairy Sci. 2017;100(7):5188–94.
75. Pan L, Yu J, Ren D, Yao C, Chen Y, Menghe B. Metabolomic analysis of significant changes in Lactobacillus casei Zhang during culturing to generation 4,000 under conditions of glucose restriction. J Dairy Sci. 2019;102(5):3851–67.
76. Monteleone I, Rizzo A, Sarra M, Sica G, Sileri P, Biancone L, MacDonald TT, Pallone F, Monteleone G. Aryl hydrocarbon receptor-induced signals up-regulate IL-22 production and inhibit inflammation in the gastrointestinal tract. Gastroenterology. 2011;141(1):237-48.e1.
77. Mentella MC, Scaldaferri F, Pizzoferrato M, Gasbarrini A, Miggiano GAD. Nutrition, IBD and gut microbiota: a review. Nutrients. 2020;12(4):944.
78. Yu K, Li Q, Sun X, Peng X, Tang Q, Chu H, Zhou L, Wang B, Zhou Z, Deng X. Bacterial indole-3-lactic acid affects epithelium–macrophage crosstalk to regulate intestinal homeostasis. Proc Natl Acad Sci. 2023;120(45):e2309032120.
79. Wang Y, Ames NP, Tun HM, Tosh SM, Jones PJ, Khafipour E. High molecular weight barley β-glucan alters gut microbiota toward reduced cardiovascular disease risk. Front Microbiol. 2016;7:129.

Publisher's Note